Tectonophysics 631 (2014) 65–86

Contents lists available at ScienceDirect

Tectonophysics

journal homepage: www.elsevier.com/locate/tecto

NACr14: A 3D model for the crustal structure of the North American Continent

Magdala Tesauro [a,*], Mikhail K. Kaban [a], Walter D. Mooney [b], Sierd Cloetingh [c,d]

[a] GeoForschungsZentrum Potsdam (GFZ), Germany
[b] USGS, United States
[c] Department of Earth Sciences, Utrecht University, The Netherlands
[d] Ludwig-Maximilians University of Munich, Germany

ARTICLE INFO

Article history:
Received 29 July 2013
Received in revised form 7 March 2014
Accepted 8 April 2014
Available online 21 April 2014

Keywords:
3D crustal model
North American continent
P-wave crustal velocity
Pn velocity
Intracrustal boundaries

ABSTRACT

Based on the large number of crustal seismic experiments carried out in the last decades we create NACr14, a 3D crustal model of the North American continent at a resolution of $1° \times 1°$. We present maps of thickness and average velocities of the main layers that comprise the North American crystalline crust, obtained from the most recent seismic crustal models within the USGS crustal structure database. However, the crustal data are unevenly distributed and in some cases discrepancies exist between published models. In order to construct a consistent 3D crustal model with three layers in the crystalline crust, we refrained from a direct interpolation of the crustal seismic parameters in the database. Instead, we implemented the following sequence of steps: 1. Definition of the geometry of the main tectonic provinces of North America; 2. Selection and evaluation of the reliability of seismic crustal models in the database; 3. Estimation of the *P-wave* seismic velocity and thickness of the upper, middle and lower crust for each tectonic province; 4. Estimation of the interpolated *Pn* velocity distribution. The resulting average velocity of the crystalline crust is mostly consistent with that of the seismic points. The main variations of the structure of the crystalline crust of North America displayed in the model can be related to its tectonic evolution. The model, available in a digital form, can be used in various geophysical applications, such as the correction for the crustal effects in gravity and seismic tomography and models of dynamic topography, in order to detect heterogeneities characterizing the underlying upper mantle.

1. Introduction

The crust is the most heterogeneous layer composing the Earth, and typically consists of several sub-layers characterized by pronounced different physical properties. Seismic studies (mainly refraction/wide-angle reflection, near-vertical incidence reflection, receiver function, and more recently ambient noise methods) provide constraints on the structure of the crust. Three dimensional (3D) crustal models have been derived from the synthesis of the seismic measurements of crustal structure, which number in the thousands. Recently, several continent-scale crustal models have been constructed using different approaches (e.g., Artemieva and Thybo, 2013; Chulick et al., 2013; Molinari and Morelli, 2011; Mooney and Kaban, 2010; Stolk et al., 2014; Tesauro et al., 2008).

The crust of North America has been studied on a full continental scale since the middle of the 20th century, decades before many other continents (Prodehl and Mooney, 2012). Seismic measurements carried out in the early 1960s provided the data coverage needed to produce the first contour maps showing the general trends of deep crustal properties (Pakiser and Steinhart, 1964; Prodehl and Mooney, 2012). These maps, based on seismic refraction/wide-angle reflection data, depict contours of crustal thickness (*H*c), average whole-crustal *P-wave* velocity (*P*c), and sub-Moho *P-wave* velocity (*Pn*). Braile et al. (1989) produced new, more detailed contour maps of *H*c, *P*c, and *Pn* for the United States and southern Canada. These maps were accompanied by the first detailed statistical analysis of crustal thickness and average crustal velocity. Mooney and Braile (1989) extended these maps to nearly the whole of North America, including regions in which little prior information was available, such as Alaska and Arctic Canada. Chulick and Mooney (2002) used a large volume of new measurements from seismic-refraction surveys, earthquake tomography studies, surface-wave analyses, and receiver functions to construct new contour maps of crustal structures and statistical analyses of the seismic structure of the crust and uppermost mantle of North America and the surrounding ocean basins. Mooney and Kaban (2010) presented an updated Moho map for North America with $1° \times 1°$ resolution using an adaptive interpolation technique applied to the most complete available database, compiled by the USGS (Mooney, in press) consisting of about 1500 determinations of crustal structure. The idea of the adaptive interpolation method is to use available surface data (topography, thickness

* Corresponding author at. Telegrafenberg A20 Potsdam D-14473, Germany. Tel.: +49 331 288 1959; fax: +49 331 288 1111.
E-mail address: magdala@gfz-potsdam.de (M. Tesauro).

http://dx.doi.org/10.1016/j.tecto.2014.04.016
0040-1951/

and properties of sediments) to reproduce the geometry of geologic features, such as circular basins or linear mountain belts. In general, the crustal structure for these geological features is determined in several places. Therefore, relationships between crustal thickness and surface parameters have been determined in a sliding window and then applied in each local area for interpolation of the measured values (Mooney and Kaban, 2010). This study also presents a detailed map of sediment thickness with a resolution of $5' \times 5'$. Using averaged borehole data, well-determined density compaction relations, and seismic profiling data, Mooney and Kaban (2010) constructed smoothed density-depth functions characterizing each type of sedimentary basin. Bensen et al. (2009) inverted surface wave dispersion curves, measured from ambient noise using 203 stations across North America, to determine a 3-D shear wave velocity model (*Vs*) of the crust and uppermost mantle beneath much of the contiguous U.S. The increasing number of the seismic station sites occupied by the USArray in the last few years (more than 1000) has provided the opportunity to reconstruct in detail the depth of the Moho and of the lithosphere–asthenosphere boundary (LAB) beneath the western United States by interpreting Ps and Sp receiver functions data (Levander and Miller, 2012), as well as to produce a new, improved 3-D shear wave velocity model beneath the central and Western U.S. up to a depth of 150 km, based on the interpretation of surface wave dispersion and receiver functions (Shen et al., 2013).

Since the crustal structures of the North American continent have been studied in more detail than other continents, there is an excellent opportunity to create a new generalized 3D crustal model showing the sub-division into discrete layers, as well as *P-wave* velocity variations within these layers. As shown in previous studies (e.g., Tesauro et al., 2009, 2012), an accurate knowledge of the crust provides an opportunity to model intraplate continental rheology and deformation caused by coupling and decoupling of the lithospheric layers. If only the average properties of the crustal structure are known, it is difficult to assess the existence of mechanical coupling/decoupling between the intra-crustal layers or to compute the lateral pressure gradients (LPG), which can drive horizontal ductile flow in the crust (Tesauro et al., 2011). Furthermore, a consistent 3-D model of the crustal structure is fundamental to the detection of heterogeneities characterizing the underlying upper mantle. In fact, reliable geophysical models (e.g., geothermal, gravity, seismic tomographic) of the upper mantle can be obtained only after subtracting the effect of the crust from the observed fields (e.g., Bedle and Van der Lee, 2009; Kaban et al., 2010; Koulakov et al., 2009). Likewise, the estimation of dynamic topography due to mantle flow beneath the lithosphere (e.g. Becker and Faccenna, 2011) requires correction for the crustal contribution to the observed topography (e.g., Boschi et al., 2010).

In this study we present NACr14, a 3D model providing the thickness, seismic *P-wave* average velocities of the crystalline crustal layers and interpolated *Pn* seismic velocities of the Northern American continent, obtained from the analysis of the most recent seismic model of the crust available in the USGS database (Mooney, in press). We did not estimate *S-wave* velocity, on account of the limited database.

2. Data

The crystalline crust is often interpreted by seismic experiment as composed of several layers, often overlain by sediments. It is commonly divided in three layers, upper, middle and lower (e.g., Bassin et al., 2000; Laske et al., 2013; Mooney et al., 1998). An almost complete dataset of the crustal parameters of the North American continent is provided by the USGS database (Mooney, in press), in which all entries are digitized from published seismic models (mainly from seismic refraction/wide-angle reflection and receiver function studies). A typical database entry (Table 1) represents a vertical column at a certain location on the Earth. For each crustal layer, the depth from the surface to the top and thickness of the layer are given, together with the *P-wave* and *S-wave* (where available) velocities of that layer. However, despite the vast amount of seismic data composing the database (>2000 data entries for the North American continent), only some of them could be used to construct the model. In fact, some data provide information only on the structure of the uppermost part of the crust or average velocities and thickness of the entire crust, which are not sufficient to assess the internal crustal subdivision. Furthermore, the spatial distribution of points is uneven, with a relatively large amount of seismic data located in the western-central part of the U.S., whereas some parts of the North America still lacks seismic experiments. There are often ambiguities in the interpretation of the entries in the seismic crustal structure database. Old interpretations may have a significant uncertainty in the estimation of seismic velocities and layer thickness. In some cases discrepancies exist between crustal models based on the same data but interpreted by different authors, while in some other cases interpretations of the intra-crustal layers, particularly seismic low-velocity zones, remain controversial. These factors may leave questionable the precise location of intra-crustal boundaries. In some studies the crust is not depicted as divided by sharp boundaries but a gradual increase in seismic velocities with depth is shown, while in other studies more than three crustal layers are detected, especially when a lowermost layer is characterized by relatively high seismic *P-wave* velocities of over 7 km/s is present. For these reasons, to obtain a consistent three layers crustal model, we did not directly interpolate the values of the crustal parameters in the database, rather we have followed the method discussed below.

3. Method

To construct a consistent model of the crystalline crust of the North American continent, providing the thickness and average velocity of the upper, middle and lower crust, we proceed through the following steps: (1.) Outlining the main North American tectonic provinces; (2.) Selection and evaluation of the reliability of the seismic models in the USGS database; (3.) Estimation of the *P-wave* seismic velocity and thickness of the upper, middle and lower crust for each tectonic province, on the basis of the analysis of the selected data points; (4.) Verification of the consistency of the results using numerical tests.

In defining the borders of the North American tectonic provinces (Fig. 1a), we took into account the age, the geographical extension of the key tectonic elements, the physiographical boundaries and the density of the data points. According to this criterion, we defined 26 tectonic provinces (Table 2). Due to uneven distribution of the data, which are concentrated in Meso-Cenozoic regions, the division of tectonic provinces is more detailed in the southwestern part of the continent (Fig. 1a).

Table 1
Example from the USGS database (Mooney, in press). The data have an identification number (ID), geographical location (Location) in latitude and longitude and several layers. For each layer the *P-* and *S-wave* velocities (Vp and Vs) are given, as well as the layer thickness (Thickness) and the depth to the top of the layer (Depth). A label (Label) indicates the type of the layer (s = sediment, c= crust and m = depth to Moho).

ID	Location	Vp (km/s)	Vs (km/s)	Thick (km)	Depth (km)	Label
1495	36.98 N	4.70	.00	2.50	.00	s
	90.25 W	6.20	.00	5.40	2.50	c
		6.50	.00	22.70	7.90	c
		7.40	.00	14.40	30.60	c
		8.10	.00	.00	45.00	m

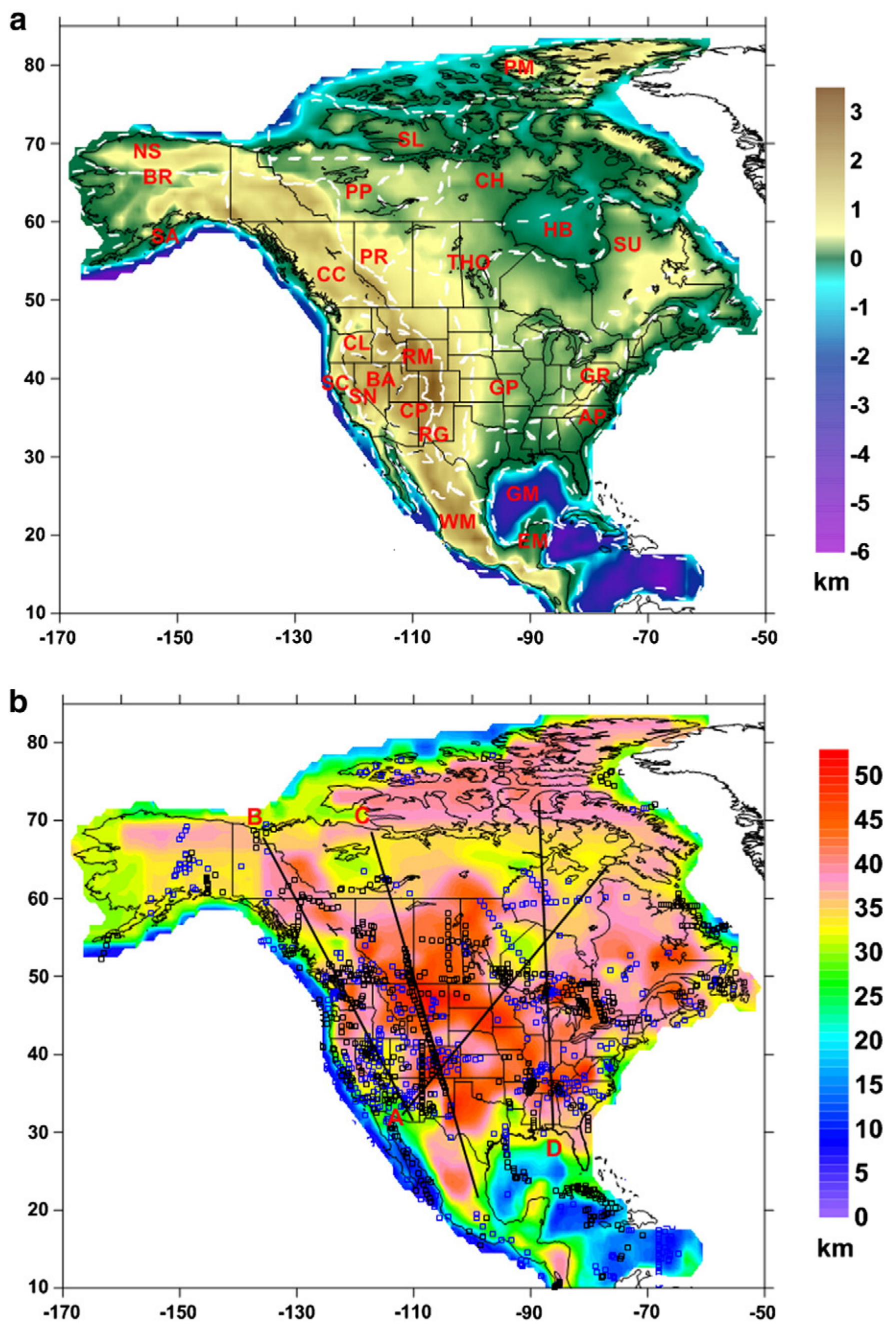

Fig. 1. (a) Topography of the North American continent. White dashed contours show the boundaries of the tectonic provinces. Red labels are: AP, Appalachians; BA, Basin and Range; BR, Brooks Range; CC, Canadian Cordillera; CH, Churchill craton; CP, Colorado Plateau; CL, Columbia Plateau; EM, Eastern Mexico; GM, Gulf of Mexico; GP, Great Plain; GR, Grenville; HB, Hudson Basin; NS, North Slope; PM, Polar margin; PP, Paleoproterozoic platform; PR, Peace River arch; RG, Rio Grande rift; RM, Rocky Mountains; SA, Southern Alaska; SC, Southern Cordillera; SL, Slave craton; SN, Sierra Nevada; SR, Snake River Plain; SU, Superior craton; THO, Trans-Hudson Orogen; WB, Williston Basin; WM, Western Mexico. (b) Thickness of the crust estimated from the USGS crustal database. Black squares show the locations of the seismic data used to construct the new crustal model. Blue squares show the locations of the additional points providing *Pn* estimates. Black lines show the locations of the cross-sections displayed in Fig. 10.

Next, we selected the points of the crustal database (Fig. 1b) and estimated the average velocity and thickness of the upper, middle and lower crust, guided by the published interpretation. For instance, in the seismic profile displayed in Fig. 2a, the crystalline crust of the Appalachians has been interpreted by Hughes et al. (1994) as composed by the upper, middle and lower crustal layers, each having specific thickness and range in seismic velocity. Therefore, we could directly estimate the average velocity in each crustal layer, in this case 6.0 km/s, 6.30 km/s and 6.75 km/s, respectively.

We could follow the same approach in other cases, such as when the crystalline crust is divided in more than 3 layers or when no internal discontinuity has been detected. Indeed, regardless of the number of layers within the crust, we were able to assign an upper, middle and lower crustal layer. For example, in the case of the Superior Craton (Fig. 2b), where the crystalline crust is divided by more than 2 internal boundaries, the three layers can still be identified. When the same seismic profiles has multiple interpretations (e.g., those crossing the Trans-Hudson orogen, interpreted by Ellis et al., 1996 and more recently by Németh et al., 2005) we used the most recent interpretation.

The results obtained in this first analysis step show a linear increase of the average velocity of the crustal layers with thickness of the crystalline crust (Fig. 3a–c). In some cases, such an increase is prevalently

Table 2
Ranges of *P-wave* velocity, with average value and standard deviation, and average thickness (percentage) for each layer of the crystalline crust (UC, Upper Crust; MC, Middle Crust; LC, Lower Crust) for different North American provinces.

Tectonic provinces	Velocity UC (km/s)	Velocity MC (km/s)	Velocity LC (km/s)	UC (%)	MC (%)	LC (%)
Polar Margin	5.80–6.15 5.97/0.11	6.30–6.60 6.46/0.1	6.70–7.0 6.86/0.1	34	33	33
Slave Craton	6.0–6.15 6.09/0.04	6.35–6.45 6.42/0.03	6.65–6.85 6.78/0.05	35	30	35
Paleoproterozoic	5.95–6.20 6.07/0.05	6.40–6.60 6.49/0.04	6.70–7.05 6.85/0.07	35–40	30	35–30
Churchill Craton	5.95–6.10 6.02/0.04	6.40–6.60 6.49/0.04	6.70–6.85 6.77/0.04	34	33	33
Trans-Hudson Orogen	5.95–6.25 6.08/0.07	6.45–6.65 6.53/0.05	6.70–7.15 6.89/0.11	35	35	30
Superior Craton	5.95–6.25 6.09/0.06	6.35–6.65 6.49/0.05	6.60–7.25 6.91/0.12	33	33	34
Grenville	5.85–6.20 6.05/0.07	6.35–6.60 6.49/0.05	6.65–7.10 6.9/0.1	33	33	34
Appalachians	6.00–6.15 6.06/0.03	6.40–6.50 6.44/0.02	6.70–6.90 6.79/0.04	33	33	34
Western Mexico	6.10–6.15 6.12/0.03	6.45–6.55 6.49/0.03	6.75–6.95 6.83/0.07	33	33	34
Eastern Mexico	5.95–6.15 6.11/0.05	6.40–6.45 6.43/0.01	6.70–6.85 6.79/0.02	33	33	34
Gulf of Mexico	6.40–6.60 6.52/0.043	0–0	0–0	100	–	–
Canadian Cordillera	5.80–6.20 5.98/0.09	6.30–6.60 6.43/0.08	6.60–6.85 6.72/0.07	33	33	34
Cuba	6.20 6.20/0.01	0–0	7.0 7.0/0.01	40	–	60
Great Plain	5.95–6.20 6.09/0.04	6.40–6.60 6.51/0.03	6.60–7.30 6.99/0.1	30	35	35
Rocky Mountain	6.0–6.25 6.16/0.05	6.40–6.70 6.6/0.06	6.90–7.30 7.14/0.09	35	35	30
Northern Rocky Mountain	5.90–6.0 5.97/0.03	6.50–6.80 6.63/0.07	6.90–7.30 7.09/0.1	40	35	25
Rio Grande Rift	5.90–6.0 5.97/0.02	6.30–6.40 6.37/0.03	6.55–6.70 6.7/0.06	40	35	25
Colorado	5.90–6.0 5.95/0.02	6.30–6.40 6.36/0.04	6.60–7.0 6.81/0.11	35	35	30
Basin and Range	5.90–6.0 5.95/0.02	6.30–6.40 6.35/0.03	6.60–6.85 6.73/0.06	38	37	25
Southern California	5.80–6.20 5.92/0.11	6.25–6.40 6.3/0.04	6.55–6.70 6.6/0.04	40	35	25
Sierra Nevada	5.90–6.10 6.0/0.04	6.30–6.40 6.37/0.02	6.80–6.90 6.83/0.03	30	35	35
Snake River Plain	5.95–6.10 6.03/0.03	6.40–6.55 6.49/0.03	6.80–7.15 6.99/0.06	30	35	35
Southern Cordillera/Columbia Plateau	5.80–6.20 5.95/0.12	6.25–6.70 6.4/0.16	6.60–7.15 6.79/0.19	28	34	38
Gulf of California	5.20–5.80 5.60/0.04	0–0	6.40–6.70 6.51/0.02	35	–	65
Southern Alaska	5.80–6.10 5.93/0.1	6.35–6.50 6.4/0.07	6.75–6.95 6.81/0.12	30	40	30
Brooks Range/North Slope	5.90–6.10 6.04/0.05	6.35–6.40 6.37/0.03	6.50–6.90 6.79/0.1	30	35	35

observed in the lowermost layer having a mafic composition, as in the Superior Craton (Fig. 4).

The linear relationship between the crustal thickness and average crustal velocity has beeny discussed in previous studies (e.g., Chulick et al., 2013) of other continents (e.g., South America). The lowermost layers of the cratons, with a more mafic composition and a relatively low temperature, have relatively high seismic velocities (≥6.8 km/s). In contrast, in young orogens, the average seismic velocity of the crust does not increase significantly with crustal thickness due to a high thermal regime and the absence of a deep mafic layer (e.g., in the Andes and Himalayan). We observed a linear increase of the thickness of the crustal layers with the thickness of the crystalline crust (Fig. 5a–c). At the same time, the percentage of the crustal thickness of each layer might be constant or vary without following a specific trend (Fig. 6a–c).

Therefore, on the base of these results, it appears that is possible to estimate for each tectonic province a characteristic range of the average crustal velocity and adopt a positive correlation with the thickness of the crystalline crust, which extends from the bottom of the sedimentary layer to the depth of the Moho. We defined the range of average velocities for specific tectonic provinces, which fits the values from the database and assumed smooth changes of the crustal parameters at the borders of the tectonic provinces. In fact, since the borders are quite uncertain, sharp changes of velocity/thickness in these areas might be artificial. Using this approach, we estimate the average velocity of the three crustal layers in each point of the grid with a resolution of $1^\circ \times 1^\circ$. In the upper crust the positive correlation between the average layer velocity and thickness of the crystalline crust is usually weaker, but, since the variability in velocities in this layer is smaller than in the others (Table 2), we preferred to estimate its average velocity by adopting the same criterion used for other layers. In some tectonic provinces, the limited amount and high variability of the data does not permit the determination of reliable relationships. In these cases the linear relation between velocity and total crustal thickness was defined using

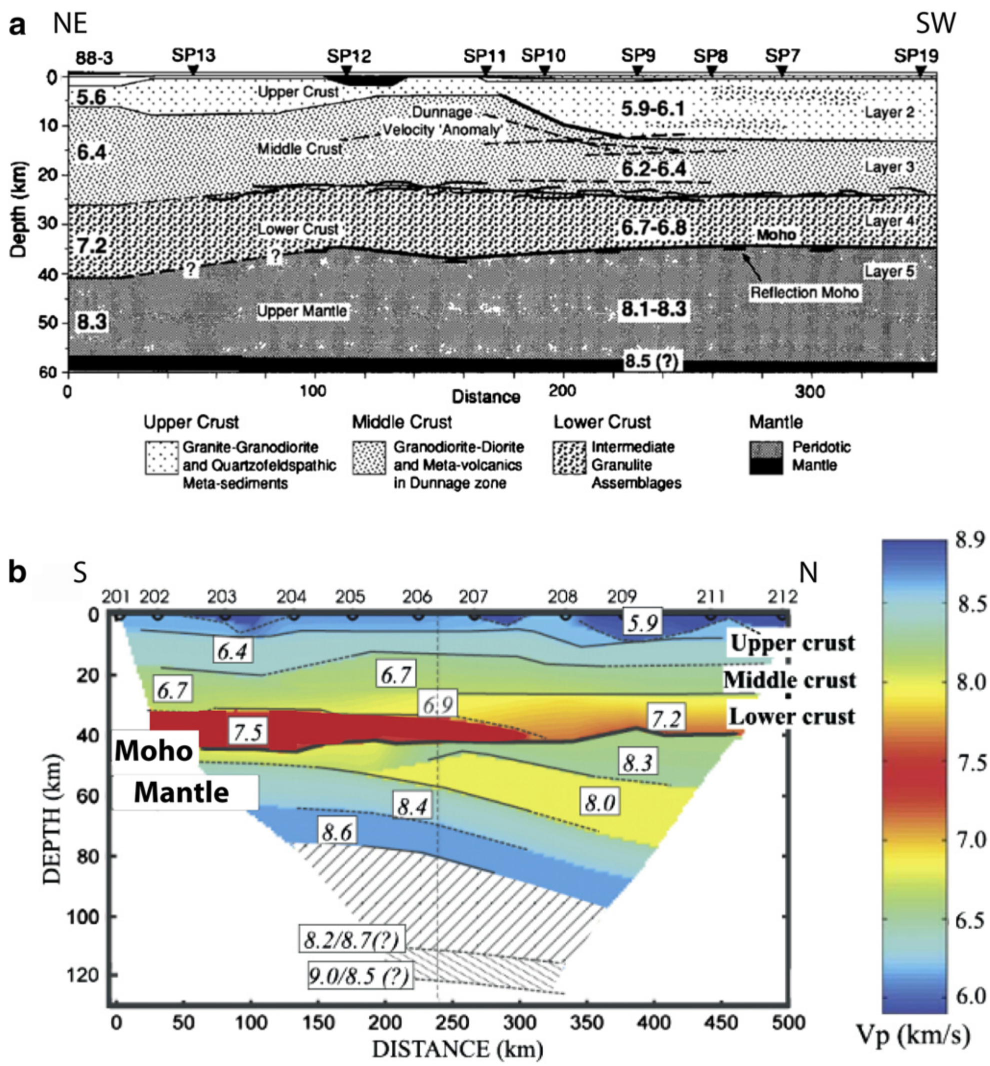

Fig. 2. a–b Interpreted crust–mantle model (a) across the Newfoundland Appalachian orogeny, modified after Hughes et al. (1994) and (b) across the western Superior province, modified after Musacchio et al. (2004).

other constraints, such as the Vp/Vs ratio estimated from receiver functions (e.g., Thompson et al., 2010). As previously stated, the relative thickness of the crustal layer does not follow a specific trend. Therefore, we estimated a uniform value of this parameter for each of the three crustal layers of the tectonic provinces (Table 2), in most cases corresponding to the averages of the data points. Using these values we could estimate thickness of the upper, middle and lower crust in each point of the grid. The choice of the parameters used to estimate the velocity and thickness of the crustal layers is discussed in Section 5. This approach does not take into account the local crustal heterogeneities, which decrease the correlation between average velocity and thickness of the crystalline crust. For this reason, we discuss in Section 6 the consistency of the results obtained through a statistical analysis and compare them with the previous interpretations of the North America crustal structure. In addition, we provide comparison of our new model with the most recent global crustal model CRUST 1.0. (Laske et al., 2013). The latter, also defined on a 1° × 1° grid, estimates Vp, Vs and density for 8 layers (water, ice, 3 sediment layers and upper, middle and lower crystalline crust). Crustal thickness data are evaluated from seismic data or using gravity constraints where the former are lacking. For cells with no local seismic or gravity constraints, statistical averages of crustal properties, including crustal thickness, were extrapolated. CRUST 1.0 was validated against new global surface wave dispersion maps and adjusted in areas of extreme misfit.

4. Sub-Moho *P-wave* velocity (*Pn*)

More seismic data are available to estimate *Pn* velocity than the database used for the estimate of the average velocity and thickness of the crystalline crust layers. Actually, even the old seismic experiments, which often do not provide the detailed seismic velocity structure in the crust, normally provide *Pn* values (e.g., in the Hudson Basin, Hobson et al., 1967). Therefore, the study area is well covered with *Pn* measurements (Fig. 1b) and we directly interpolate them with ordinary kriging on a uniform 1° × 1° grid, after exclusion of outliers with values either lower than 7.6 km/s or over 8.4 km, using standard commercial softer (SURFER). The uncertainties of the results obtained depend on those of the initial values. The contour map displayed in Fig. 7 is similar to that presented by Chulick and Mooney (2002), with the mean value slightly larger, due to the inclusion of data from the stable continental interior (Table 4). A systematic difference occurs between the *Pn* values for the Meso-Cenozoic Cordillera (<8.0 km/s) as compared with the Precambrian regions (>8.0 km/s).

Such a difference, present in the area of the Rocky Mountains, is also found in *S-wave* velocity models (e.g., Bensen et al., 2009; Yuan et al., 2011) and is closely correlated with the thermal state of the lithosphere. This lateral change is sharper in the *Pn* model of Zhang et al. (2009) and occurs along the eastern border of the Rocky Montains. The lower *Pn* velocities correspond to higher lithospheric temperatures (e.g., Mooney

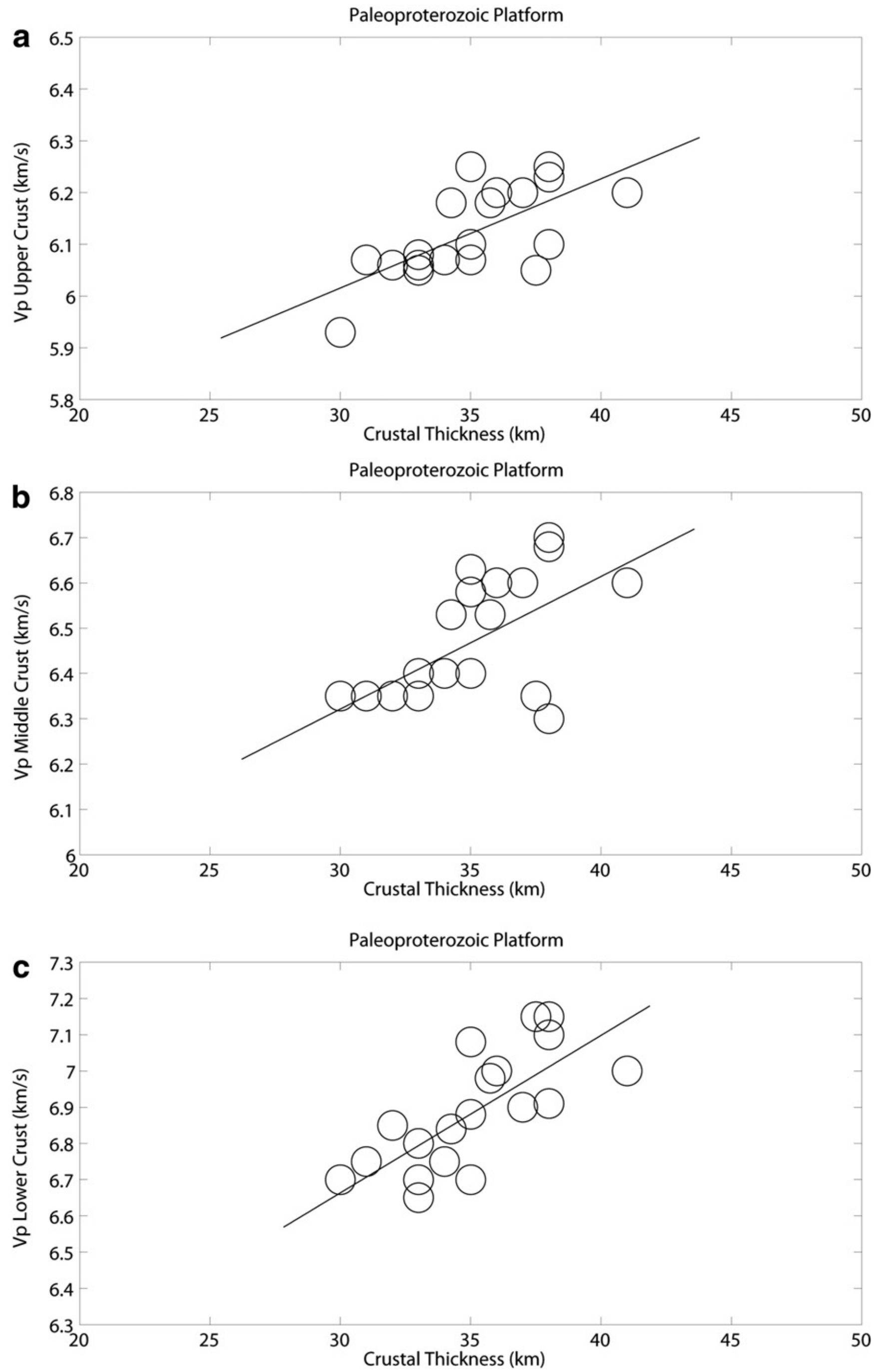

Fig. 3. (a–c) Relationships of the average *P-wave* velocity (km/s) in (a) the upper; (b) middle and (c) lower crust versus thickness of the crystalline crust (km) for the Paleoproterozoic platform (see Fig. (1a–b) for location). The values are positively correlated.

and Braile, 1989). As in the model of Buehler and Shearer (2012), low *Pn* values (~7.8 km/s) are observed beneath the Snake River Plain, Basin and Range and the western edge of Colorado. In contrast with this study, a slight increase of *Pn* values to 7.9–8.0 km/s is found beneath Sierra Nevada and California. The northern part of the Canadian Shield (e.g., in the Slave province) is sparsely covered by data, but the interpolated *Pn* values (~8.15 km/s) are in agreement with those of Fernández-Viejo and Clowes (2003).

The Hudson Bay and the northeastern part of the Canadian Shield are characterized by the largest *Pn* values (>8.2 km/s), according to the study of Hobson et al. (1967) and Berry and Fuchs (1973). High *Pn* values are estimated in the southern part of the Trans-Hudson Orogen and the eastern part of the Great Plains (Fig. 7), while in the model of Zhang et al. (2009) they are observed in the northwestern boundary of the Mississippi Embayment and North and South Carolina. On the other hand, the high values (~8.3 km/s) estimated in the central part of Mexico are not robust features, being constrained by only two data points. The low *Pn* anomaly in the northern part of Mexico is likely the result of extrapolation of the low values (<7.8 km/s) observed in the Gulf of California and in the Basin and Range. As in the model

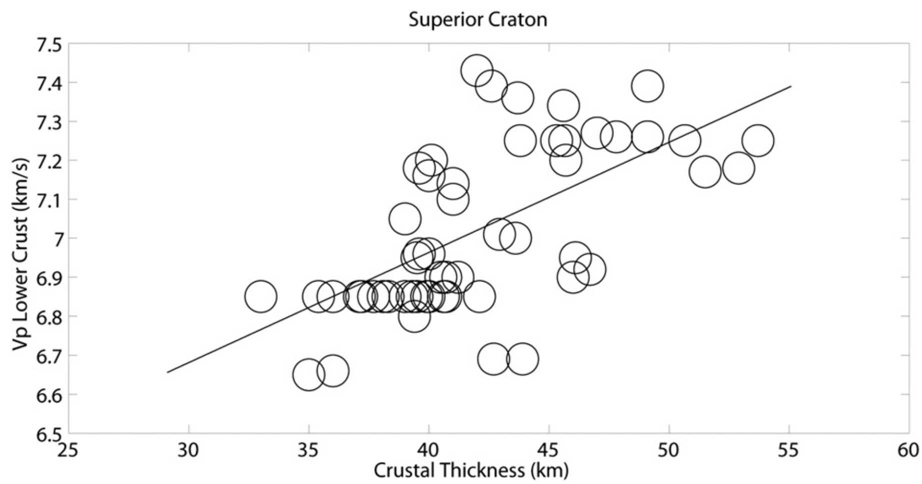

Fig. 4. Relationships of the average *P-wave* velocity (km/s) in the lower crust versus thickness of the crystalline crust (km) for the Superior Craton (see Fig. (1a–b) for location). The values are positively correlated.

of Zhang et al. (2009), relatively low velocities within the NA cratons (~8.0 km/s) are observed beneath the central part of the Great Plains and along the eastern edge of the craton.

5. Main parameters and reliability of the new crustal model

The average velocity and thickness of the three main layers of the crystalline crust and of the entire crystalline crust of North America are displayed in Figs. 8(a–d) and 9(a–d) and along four cross-sections in Fig. 10(a–d). In the off-shore regions, such as Gulf of Mexico and Gulf of California, and beneath Cuba the crystalline crust is thinner and consists of only one or two layers (Table 2).

The top of the crystalline crust is not uniquely defined by seismic data. In Western Europe it usually corresponds to the depth where the seismic velocity reaches 5.4–5.6 km/s, whereas in most of the East European Platform, where the uppermost part of the crust is characterized by a thick layer of carbonates, the top of the basement is usually associated to a *Vp* ~ 5.8 km/s (Artemieva and Thybo, 2013). The value 5.8 km/s was chosen by Chulick et al. (2013) to identify the top of the basement in the South American continent, being higher than the velocity in most sedimentary rocks and lower than the minimum velocity (>5.9 km/s) found in granitic rocks. Given the ambiguity in identifying the thickness of sediments for each individual data point, in NACr14 the minimum average velocity of the upper crust corresponds to the value of 5.8 km/s and 5.5 km/s in the on-shore and off-shore regions, respectively (Fig. 8a). However, values >6.0 km/s are usually observed in Proterozoic and Archean regions. In the middle crust the minimum values (~6.2 km/s) correspond to off-shore regions, while the largest ones (>6.6 km/s) are found beneath the Rocky Mountains and in Montana close to the Canadian border (Fig. 8b). In the lower crust (Fig. 8c), velocity values over 7.0 km/s, characterizing most of the Proterozoic platform of the U.S., the Wyoming craton and part of the Superior craton, are due to the presence of the lowermost high velocity layer (seismically defined '7.x layer', e.g., Gorman et al., 2002), reflecting the tectonic and magmatic processes associated with continental rifting, collision, subduction and other thermal lithospheric evolution, and its occurrence also provides information on the nature of the underlying mantle. However, there is no systematic geographical and age information on this process of crustal growth, while information on the geographical extent of this high velocity layer is very spotty (Mahan et al., 2012). The average velocities in the crystalline crust (Fig. 8d) have been estimated as a weight average of the velocities of the intra-crustal layers and are mostly influenced by the velocity variability within the middle and lower crust, being the velocity within the upper crust and the thickness of the layers more uniform. Our model, similarly to the shear wave model of Bensen et al. (2009), displays a trend of velocities higher in the eastern than in the western US. The thickness of the layers is quite uniform with values mostly concentrated between 11 and 13 km (Fig. 9a–c). In some regions, such as those subjected to pronounced tectonic extension (e.g., Basin and Range), the lower crust is <10 km, being reduced to 25% of the crystalline crust (Table 2). The thickness and average velocity of the intra-crustal layers show stronger lateral variations than CRUST 1.0.

The uncertainties of the crustal model presented depend on both the quality of the seismic data selected and on the reliability of the assumptions used. The uncertainty of the original data on the average *Vp* in each of the three layers, depending on the approach used in the seismic interpretations (e.g., Majdański, 2013), is usually ± 0.1–0.2 km/s, but can be locally even higher, whereas the uncertainty in thickness can be as large as ca. ±5 km. These uncertainties arise from several factors, such as the field survey method, the spatial resolution of the survey (e.g., the spacing of the shot points and the recording stations), and the analytical techniques used to process and interpret the data. We verified the reliability of the assumptions by comparing the weighted average velocities of the crystalline crust of NACr14 with those estimated in the data points composing the database for the area where the largest amount of points are located (70.75 N, 134.75 W, 10.25 N, 40.25 W) and for three large tectonic provinces (Fig. 1a).

The results, displayed in Fig. 11(a–d), show that the values of NACr14 are distributed in a narrow and more uniform range than those of the data points. The data points are scattered in a relatively large range (6.0–6.90 km/s) and have two small peaks (~10% of values) at 6.30 and 6.50 km/s (Fig. 11a), corresponding to areas with low (e.g., Basin and Range) and high average velocities (e.g., the regions characterized by the "7.x layer" in the lowermost part of the crust). In contrast, in NACr14 more than 50% of values are in the range of 6.40–6.50 km/s (Fig. 11a), which are typical values of the continental crust. As discussed below, for specific tectonic provinces, the differences observed are likely due to a variety of factors, such as: (1) the unequal distribution of the data points; (2) the possible presence of outliers between the data points; and (3) some strong crustal heterogeneities not taken into account by our model.

In the Colorado Plateau, the average values of the crustal model and those of the data points have very similar mean and are distributed around the same mean peak (6.35 km/s) (Fig. 11b). The similarities between the two trends are due to the relatively uniform distribution of the data points (Fig. 1b) and the absence of strong crustal heterogeneities in this region. The few anomalously low (<6.25 km/s) and high (>6.50 km/s) values are due to data outliers.

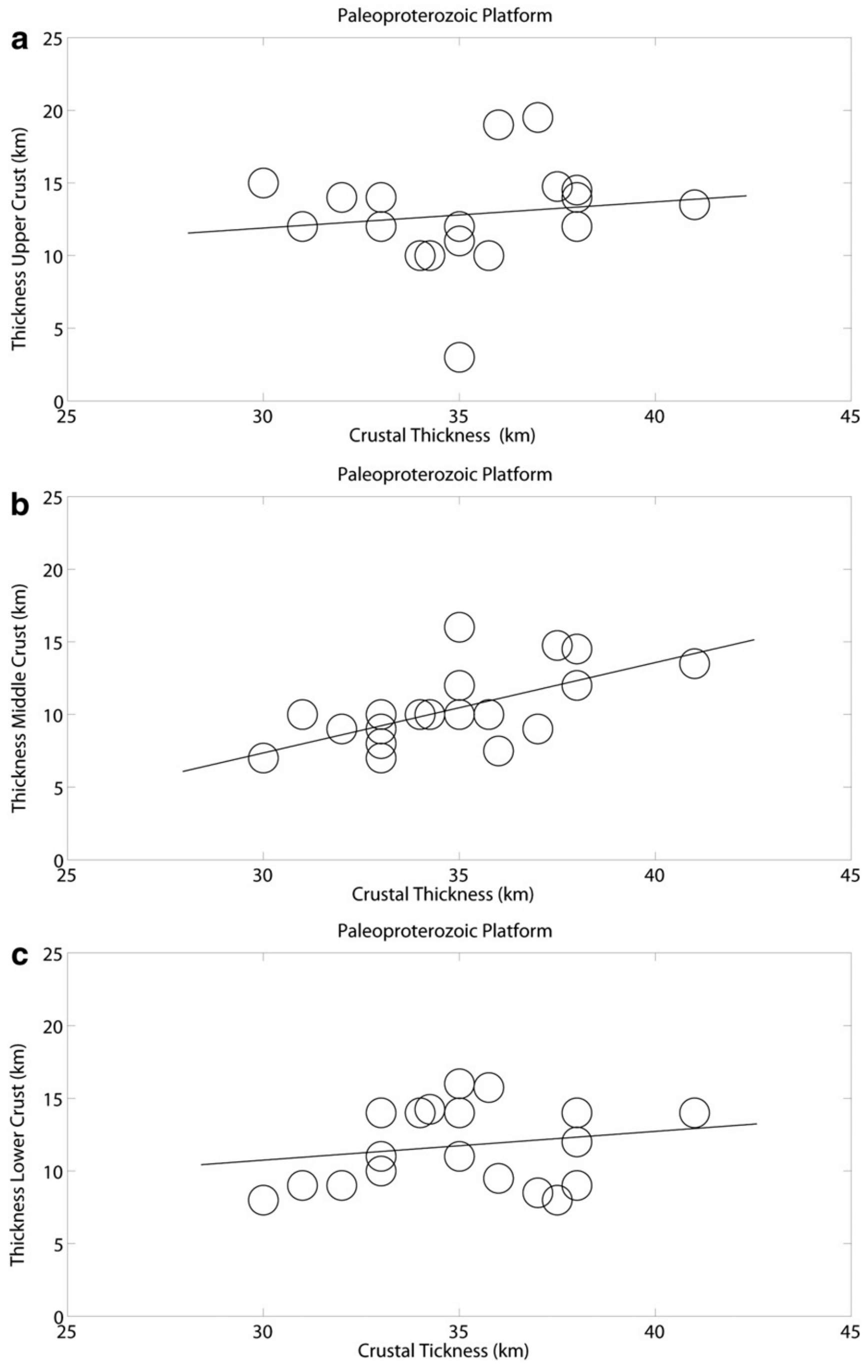

Fig. 5. (a–c) Thickness (km) of the (a) upper; (b) middle and (c) lower crust in the Paleoproterozoic platform (see Fig. 1(a–b) for location). The values are positive correlated with the thickness of the crystalline crust (km).

In the Rocky Mountains the data points are distributed in a larger range (6.1–6.9 km/s) with respect to NACr14 (6.35–6.70 km/s) (Fig. 11c). However, a large percentage of values (>40%) of both datasets are distributed between 6.55 and 6.65 km/s, on account of the '7.x layer', characterizing this region. In this tectonic province the mean value of our model is larger than that of the compiled data points by ~0.049 km/s on account of the higher percentage of values having an average velocity >6.6 km/s. As in case of the Colorado plateau, the extremely low (<6.35 km/s) and high (>6.75 km/s) values likely represent outliers, rather than strong crustal heterogeneities, as they are very different from other points observed in the same area.

The strong heterogeneity of the crustal structure of the Superior craton is reflected by the relatively large range of values (Fig. 11d) of NACr14 (6.2–6.7 km/s) and of the data points (6.2–6.9 km/s). In our model 35% of values are distributed around the mean peak at 6.5 km/s and on average are lower than that of the data points by ~0.068 km/s. The latter, being unequally distributed in this region (Fig. 1a–b), show values mostly scattered in their range (Fig. 11d). The largest values of the data points (>6.65 km/s) are observed in the Lake Superior and surrounding areas, where NACr14 shows high seismic velocities as well (Fig. 7d). Such anomalous high values are due to local bodies having an ultramafic composition (Shay and Trehu, 1993). The highest peak in data points distribution (~20% of values) at 6.30 km/s (Fig. 11d) is

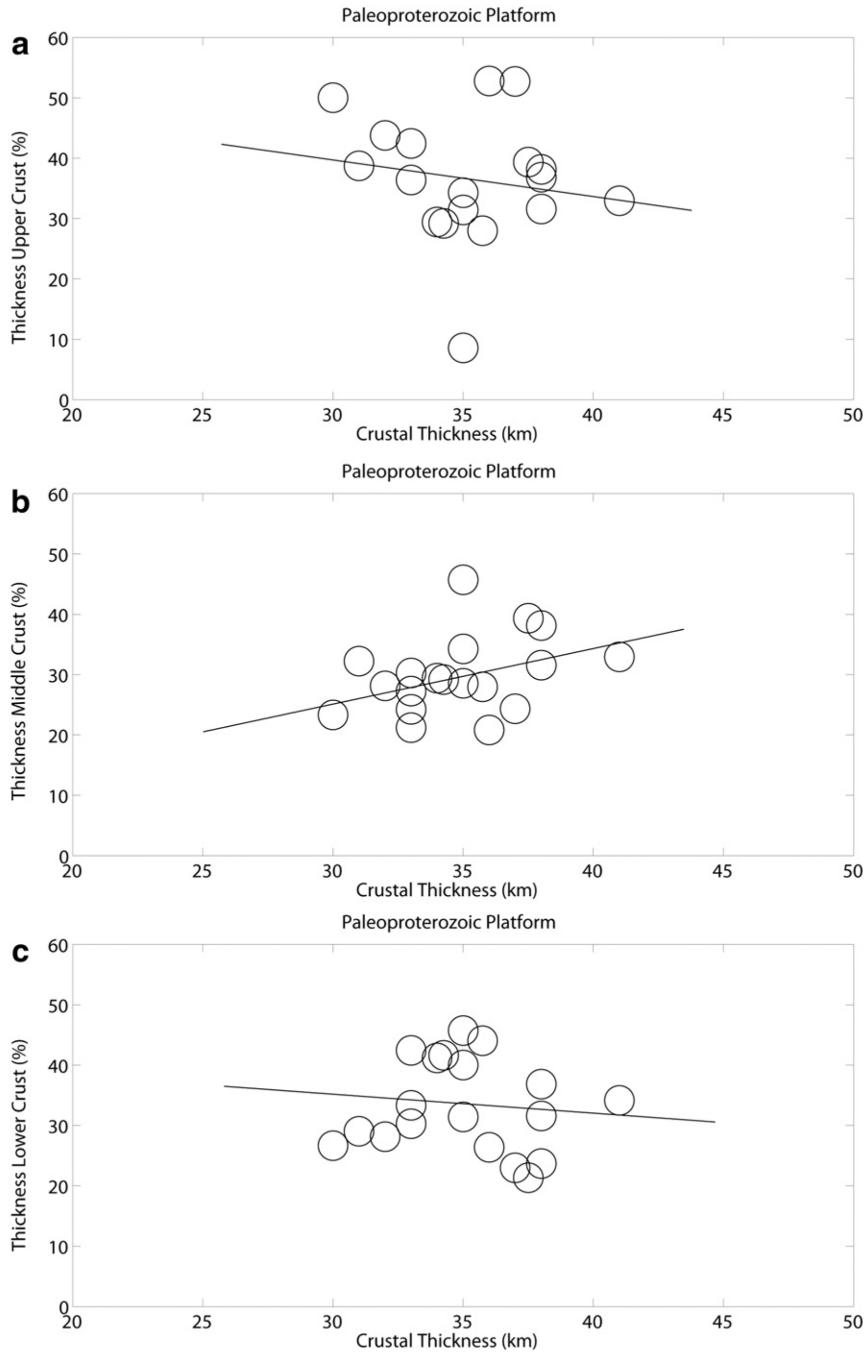

Fig. 6. (a–c) Thickness (relative to the thickness of the crust) of the (a) upper; (b) middle and (c) lower crust, respectively, in the Paleoproterozoic platform (see Fig. 1a–b for location). The values do not show any correlation with the thickness of the crystalline crust (km).

representative of the northwestern part of the craton, close to the Hudson Basin, where old seismic experiments (Hall and Hajnal, 1969) estimated low velocity values, while NACr14 suggests the values slightly larger (Fig. 7d).

A more detailed statistical analysis of the intra-crustal velocities of NACr14 is presented in the next section.

6. Structure of the crystalline crust of the North American continent

In order to investigate where the model reproduces more realistically the crustal structure, we evaluated, for each tectonic province, the average velocities of the intra-crustal layers using the values provided by the seismic data points and those of: (1) our new model and (2) CRUST 1.0 at the same points and calculated their differences (Table 3 (a–c)). This analysis demonstrates that NACr14 fits the values of the seismic points better than CRUST 1.0 for all three crustal layers. The largest misfit for either model (>0.3 km/s) is observed in the upper crust and might be related to the ambiguity in identifying the top of the basement in each individual data point. In particular the seismic points located close to the coastline (e.g., those located along the southwestern coast of Mexico) often show a sudden strong velocity drop in the uppermost layer, below the threshold defined for the off-shore regions (5.5 km/s), which is not taken into account in NACr14 and CRUST 1.0.

There exists no direct relation between the fit and the number of seismic data points in each tectonic province, nor with the geographical size of the latter. In fact, generally a good fit exists in several tectonic provinces of the Canadian Shield with only few seismic experiments (Table 3(a–c)). On the other hand, having a large number of seismic

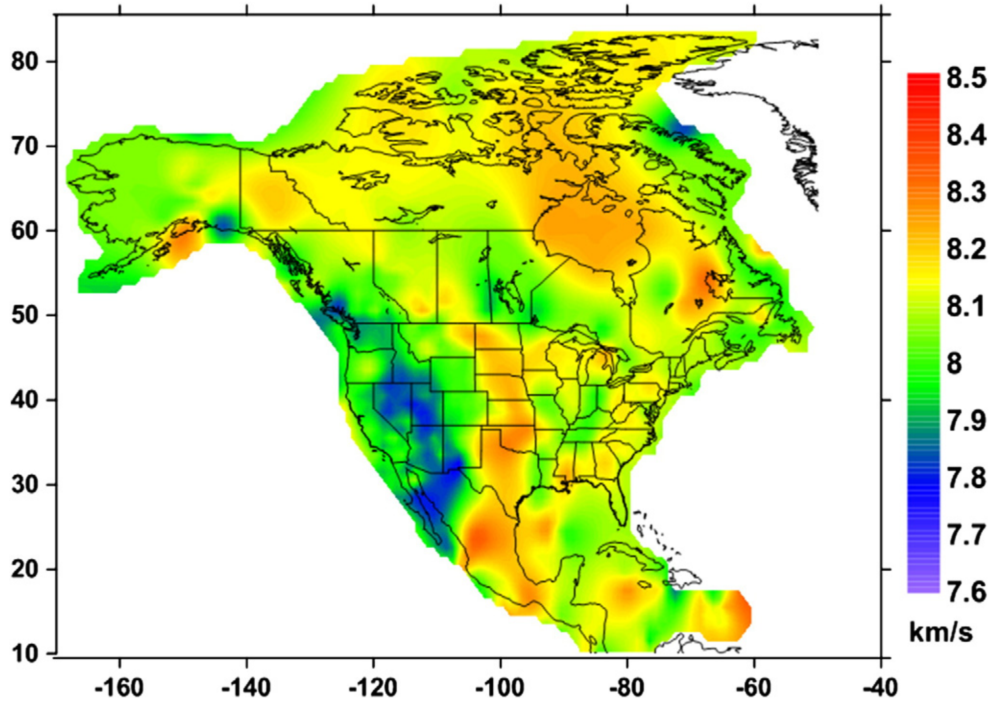

Fig. 7. Sub-Moho *P-wave* velocity, *Pn* (km/s).

data in any tectonic province does not necessarily imply a better fit of the data by the new crustal model due to the high velocity variability of the data. Large differences between the average of the seismic data and of NACr14 (>0.15 km/s) might be related, as discussed before, to the presence of 'outliers' or to the data points corresponding to local crustal heterogeneities, which are not considered in NACr14. In addition, we should also take into account discrepancies between different interpretations given for the original seismic profiles located in the same areas. For this reason, the average velocities of the intra-crustal layers estimated in the seismic data points do not always refer to the same layer. In this case, the differences between the seismic data and the model reflect different geological interpretations of the crustal structure along seismic sections. Below we discuss in more detail the results of this statistical analysis and the main peculiarities of the structure of the crystalline crust of North America in relation with tectonic evolution of the tectonic provinces.

The crust of southern **Alaska** is composed of several anomalous low and high velocity layers, corresponding to fragments of the oceanic crust (basalt, gabbro, and metamorphosed equivalents) and mantle interlayered with sedimentary and metasedimentary rocks (Fuis et al., 1991). To the north, the crustal structure of the **Brooks Range**, a west trending north vergent orogenic belt that formed along a part of the North American continental margin, is influenced by the Mesozoic southward dipping subduction zone (Moore et al., 1994). The complexity of the structures of these tectonic provinces makes more uncertain the depth of the intra-crustal boundaries (and consequently the intracrustal average velocity) in the seismic data points. The new model, showing intermediate velocities values (Fig. 9a–d), overestimates the velocity in the middle crust of the Brooks Range (~ − 0.2 km/s), which is anomalously low (Table 3b), but at the same time underestimates the velocity in the lower crust (0.15 km/s). The average velocity of the crystalline crust in Southern Alaska is slightly higher (~6.46 km/s) than that of the Earth continental average (Christensen and Mooney, 1995) and it smoothly increases to the north according to the previous studies (e.g., Fuis et al., 1991). In contrast, 300 km south to the **Brooks Range**, CRUST 1.0 shows a sharp velocity decrease from south (~6.55 km/s) to north (6.33 km/s).

To the northeast, the crust of the **North American polar margin**, formed during the Cretaceous by rifting and counterclockwise rotation when Alaska and Siberia separated from the Arctic Islands (Sweeney, 1985), is relatively thick (35–40 km, Mooney and Kaban, 2010) and its velocity corresponds to rocks with granitic and basaltic composition (Hajnal, 1992). According to these previous results, we associate intermediate velocity values to the crustal layers having similar thickness (Fig. 9a–d and Table 2). Although in the seismic interpretation of the original data (Hajnal, 1992) the middle crust is absent, we still assume a three layers division in this region, as in other areas, since the crystalline crust is relatively thick (>35 km). We compensate the insertion of the middle layer by associating to the lower layer a velocity lower (~0.16 km/s) than that estimated by the seismic experiments (Table 3(a–c)).

The **Canadian Cordillera**, includes five major morphological belts (from east to west, the Foreland belt, the Omineca belt, the Intramontane belt, the Coast belt and the Insular belt), which represent the product of a wide variety of tectonic processes (e.g., Hardebol et al., 2013). The new model, in agreement with previous studies (e.g., Clowes et al., 2005; Creaser and Spence, 2005; Kanasewich et al., 1994), shows generally low velocities (Table 3 (a–c)), increasing in the lower crust up to values of ~6.8 km/s (Fig. 10b). The low average velocity of the crystalline crust (6.3–6.4 km/s, Fig. 9d) is possibly related more to the high heat flow of the region (>100 mW/m^2, Lewis et al., 2003), than to compositional anomalies (e.g., Hammer and Clowes, 2004). Seismic data acquired across the southeastern Canadian Cordillera (e.g., Clowes et al., 2005; Zelt and White, 1995; Zelt et al., 1993) have revealed a continuous increase in the crustal seismic velocities westward from the Foreland belt to the Insular belt, possibly related to the decrease in felsic crustal components with a corresponding increase in mafic content. These velocity variations, observed at the boundaries of the belts composing the Canadian Cordillera, are not reproduced by NACr14 (Fig. 9c), since they do not show a clear relation with changes of the crustal thickness.

The **Columbia Plateau** located southwest of the Canadian Cordillera, is one of the largest flood basalt provinces in the world (e.g., Catchings and Mooney, 1988a). The crust contains a lower crustal '7.x layer' (~7.5 km/s) that is thickened in the central part and causes a local deepening of the Moho (Catchings and Mooney, 1988a). Schmandt and Humphreys (2011) suggest that the '7.x layer' might represent an obducted oceanic terrane. In agreement with these results (Table 3(a–c)), NACr14 shows a high average velocity of the crystalline crust (~6.60 km/s), on account of the relatively thick and high velocity middle (>6.55 km/s) and lower (>7.0 km/s) crustal layer (Figs. 8b–c, 9b–c and 10b). The high velocity layer in the lowermost part of the crust, identified also in the *S-wave* model of Porritt et al. (in press), extends south of the Columbia Plateau in east-central Oregon, a region dominated by continental flood basalts and extensional faulting, that is associated with the subduction of the Juan De Fuca plate (Catchings and Mooney, 1988b). This '7.x layer' (~7.45 km/s) consists of an intrusive mixture of mantle-derived magmas with the preexisting lower crust if continental extension and rifting have been active beneath east central Oregon. Alternatively, this layer may have originated from magmatic crustal underplating, which effectively maintained a thick crust despite large amounts of crustal extension (Catchings and Mooney, 1988b). The new model shows for east-central Oregon a crustal structure similar to that of Columbia Plateau, having slightly lower velocity (Fig. 9d), due to the shallower Moho depth (Mooney and Kaban, 2010).

In southern Oregon beneath the **High Lava Plains**, close to the border of the Basin and Range province, our model shows a sharp reduction in the average velocity of the crystalline crust (from 6.55 km/s to 6.35 km/s), mostly due to the decrease of velocity in the lower crust (Figs. 9c and 10b). Low crustal velocities in this region, identified in previous studies (e.g., Eagar et al., 2011; Wagner et al., 2012), are likely due to a presence of partial melt, according to very high Poisson's ratios (~0.320), low crustal S wave velocities (Wagner et al., 2012), high heat flow values (Blackwell and Richards, 2004), high crustal temperatures (Bouligand et al., 2009) and high lower crustal conductivity (Patro and Egbert, 2008). CRUST 1.0 shows a similar sharp velocity variation, but does not reproduce the anomalous high velocity in the Columbia Plateau.

The **Basin and Range** province is characterized by high heat flow (~90 mW/m^2, Blackwell et al., 1991), high lower crustal

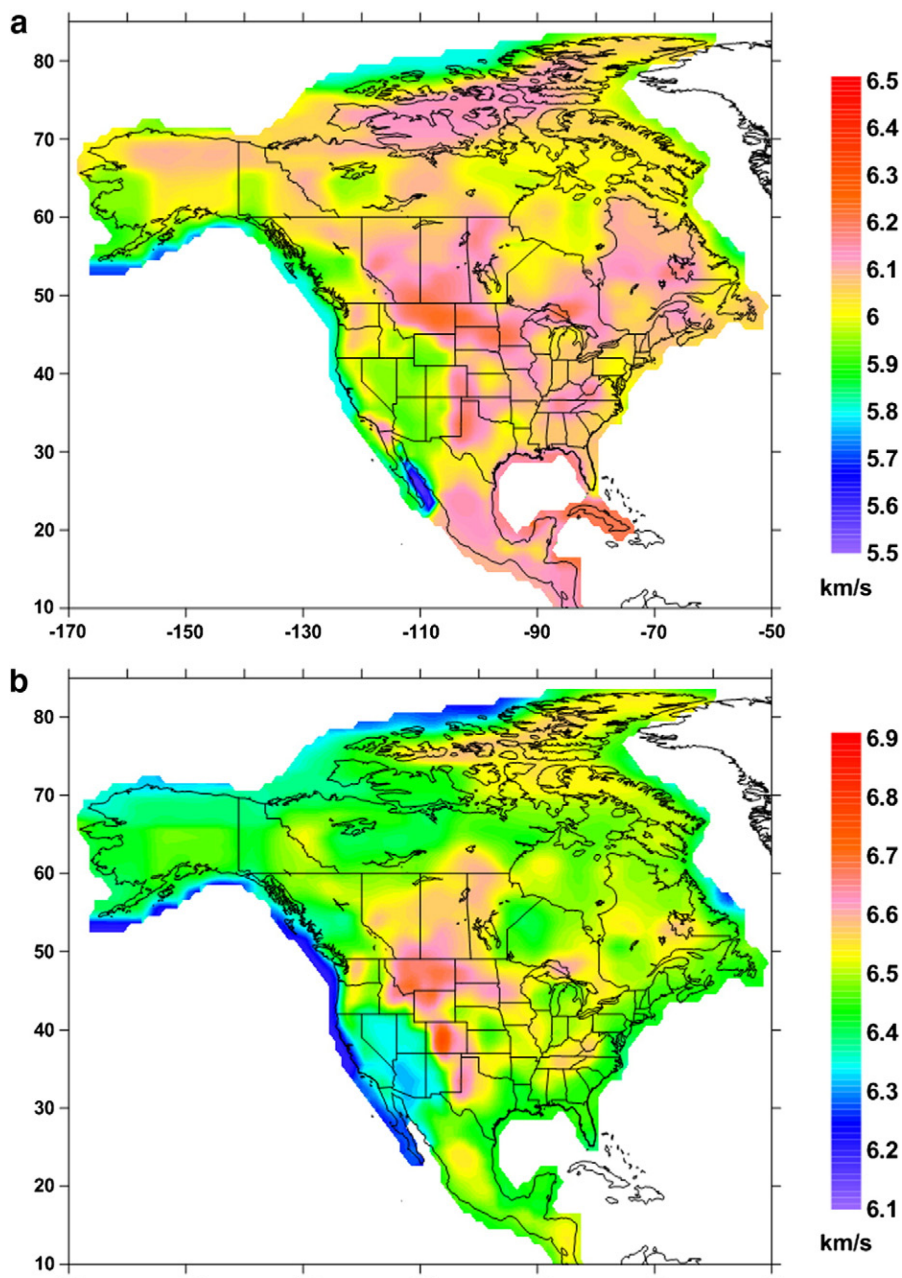

Fig. 8. (a–d) Average *P-wave* seismic velocity of the (a) upper; (b) middle; (c) lower and (d) whole crystalline crust (km/s) of the North American continent.

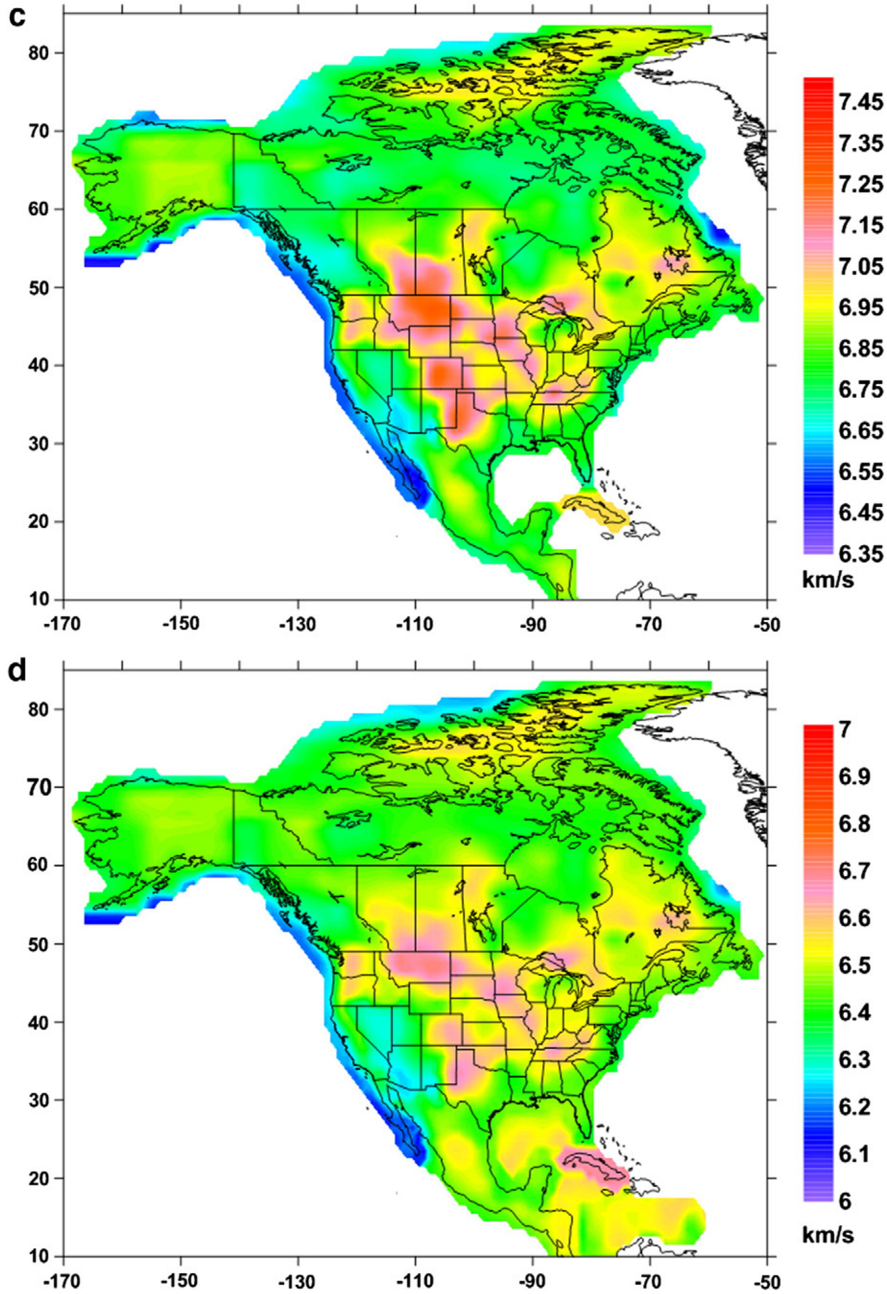

Fig. 8 (*continued*).

conductivity (Meqbel et al., in press) and thin crust (~30 km, Braile et al., 1989; Mooney and Kaban, 2010), which result from the Cenozoic extension, accompanied by intrusive an extrusive igneous activity (e.g., Steward and Carlson, 1976) and crustal thinning (e.g. Smith et al., 1989). In our model the upper and middle layers comprise most of the crust (75%), since crustal thinning has affected mainly the lower crust. The upper and middle crustal layers show low average velocities (5.95 km/s and 6.35 km/s, respectively, Table 2 and Figs. 9d and 10b), as already observed in previous studies (e.g., Catchings and Mooney, 1991). In contrast, the thin lower crustal layer is more structurally complex, having an unusually high velocity (7.4 km/s, Catchings and Mooney, 1991), which has been identified as mantle in some previous studies (e.g., Stauber and Boore, 1978). Such a "7.x layer", thickening from central to northwestern Nevada, up to 7 km, was interpreted as the addition of mantle-derived melts to the base of the crust during the Basin and Range rifting (Catchings, 1992). On the other hand, the thickening of the "7.x layer" is in contradiction with the minor amount of upper-crustal extension of western Nevada (30%, Colgan et al., 2006), respect to the central part of Nevada (>50% Smith et al., 1991). More recently, Lerch et al. (2007) observed a slight increase of lower crustal velocities from east to west, up to the maximum of 6.85 km/s across the northwestern Basin and Range, without identifying the "7.x layer". In NACr14 we did not consider the influence of the "7.x layer", since it was detected only in a limited geographical area and the lower crust shows a velocity of ~6.75 km/s in the central part of the Basin and Range and decreases to ~6.6 km/s in its southern part. The fit of the seismic data points is good in the Basin and Range, while in the Sierra Nevada NACr14 shows lower velocities in all three crustal layers (Table 3(a–c)). However, in the latter province, the velocity is constrained by only two data points (Fig. 1b).

Crustal structure of the **Rio Grande Rift**, a Cenozoic extensional feature superimposed upon preexisting zones of crustal weakness, located east from the southeastern Basin and Range, is very similar to the Basin and Range, as also observed in previous studies (e.g., Sinno et al., 1986). Indeed, this region is characterized by anomalous high heat flow (>100 mWm^2, e.g., Swanberg, 1979) and merges with the broader extensional region of the Basin and Range province in southern New Mexico (Smith et al., 1989). As in the North American Polar margin, we prefer to assume a three layers' crustal structure, although the few seismic data were interpreted by a two-layer crustal model (Sinno et al., 1986).

West of the Basin and Range, the crustal structure of **California** is quite heterogeneous, being characterized in the northern and central part by low velocity in the upper crust and by the middle and lower crust composed of rocks having intermediate velocities (Eaton, 1966). The new model shows intermediate velocities of the crustal layers of California region (Fig. 9a–d; Table 2), but it does not display anomalously high velocities in the central part of the Great Valley, estimated in the previous studies of Colburn and Mooney (1986) and Holbrook and Mooney (1987), since they are not correlated with crustal thickness variations. In the **Gulf of California**, NACr14 shows low velocities of the two crustal layers (<6.0 km/s and ~6.60 km/s) composing the thin crust (<20 km) of this region. However, as in the southern part of California, the velocities according to the original off-shore seismic data (Phillips, 1964) are anomalously low in the upper layer (Table 3(a–c)), reflecting a transition to the oceanic crust.

Northeast to the Basin and Range, in the **Snake River Plain**, the crust thickens from 30 to 35 km (Braile et al., 1989; Mooney and Kaban, 2010), but the upper crust becomes thinner respect to the other layers and beneath the Yellowstone caldera its velocity is reduced (<6.0 km/s), possibly due to a hot body of granitic composition, partially melted (e.g., Smith et al., 1982). In contrast, the middle and lower crustal layer are thicker and have velocity larger than the northern Basin and Range (e.g., Smith et al., 1982), possibly on account of an intrusion of a mafic body (e.g., Sparlin et al., 1982). In NACr14 the percentage of the thickness of the upper crust is lower than those of the middle and

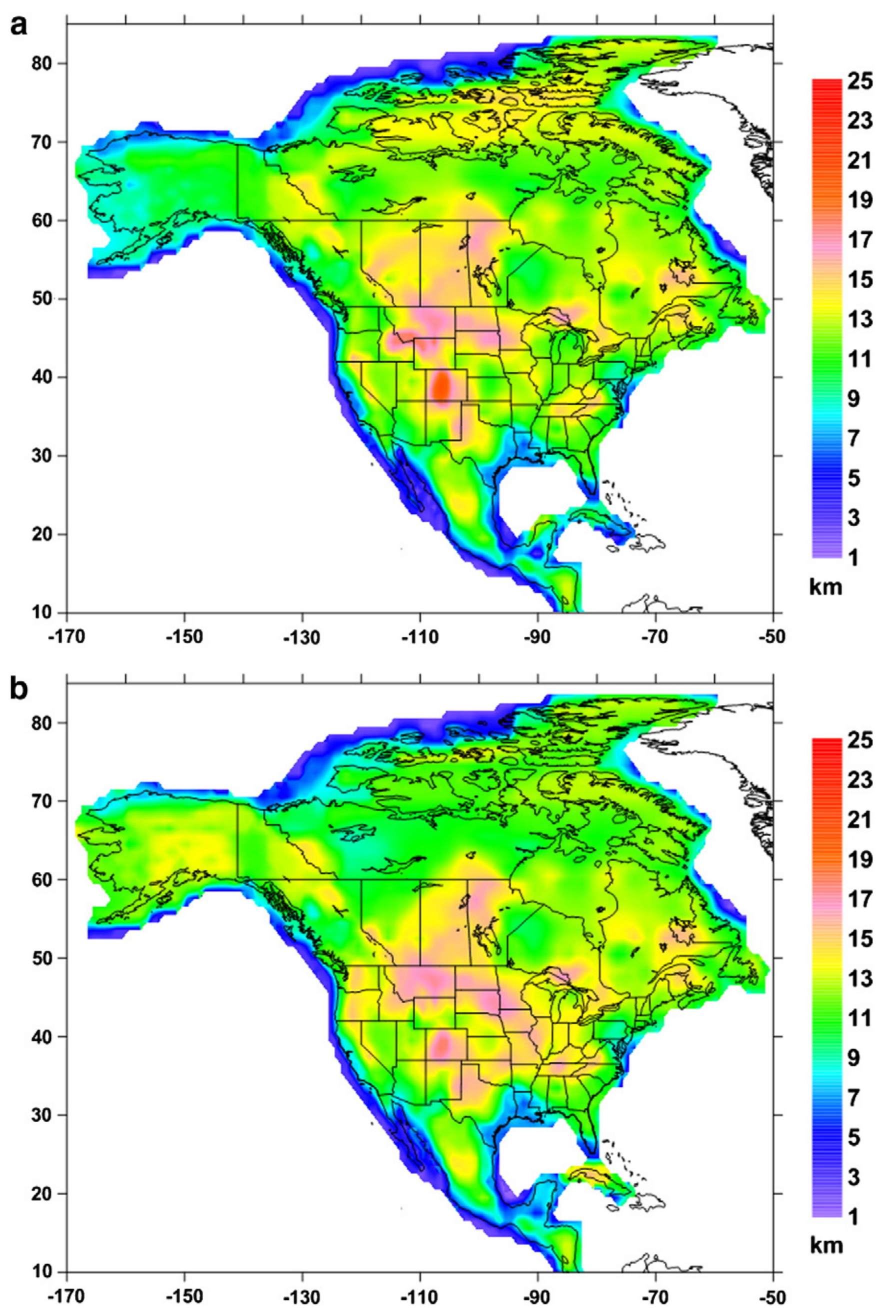

Fig. 9. (a–d) Thickness (km) of the (a) upper; (b) middle; (c) lower and (d) whole crystalline crust of the North American continent.

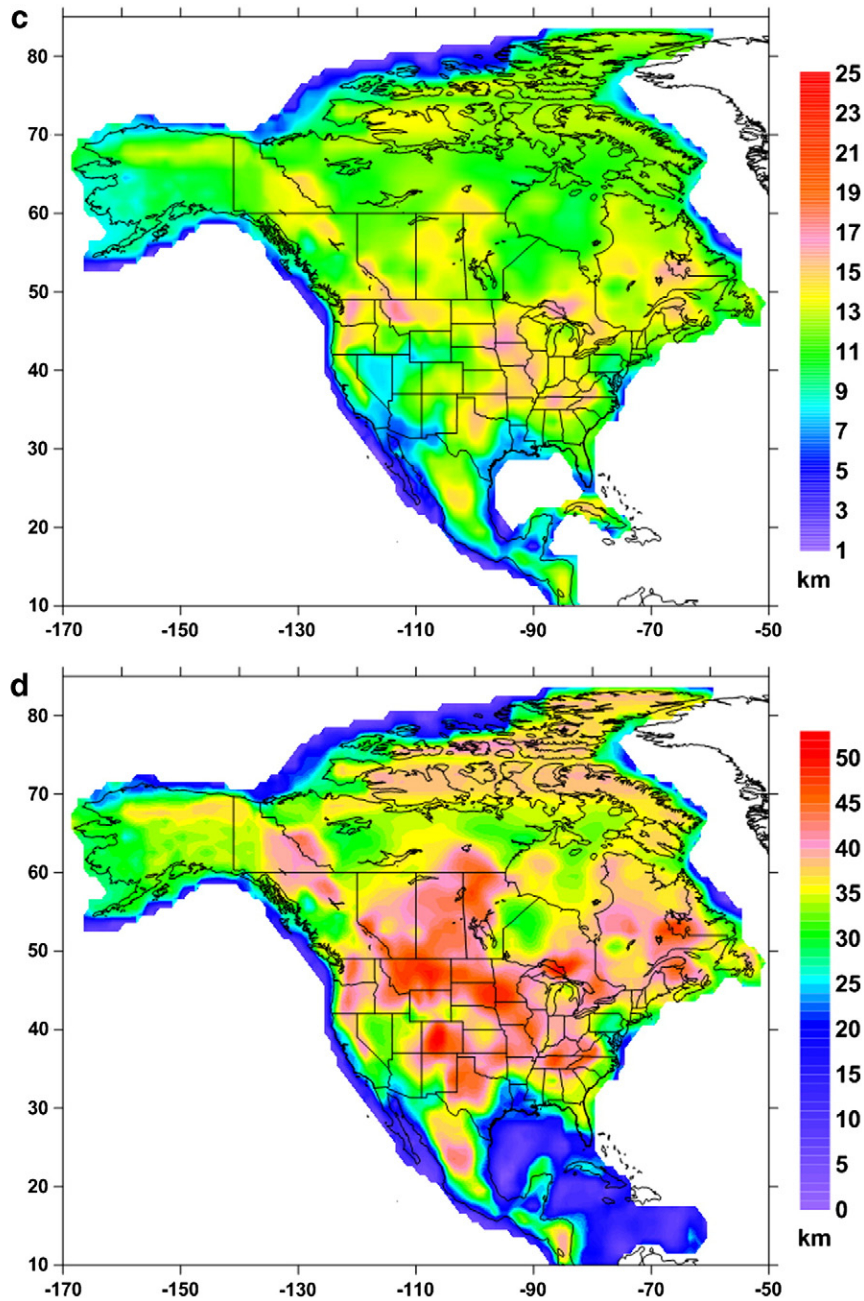

Fig. 9 (*continued*).

lower crust (Table 2 and Fig. 10b), while the ranges of velocities associated to the crustal layers result in an average velocity of the crystalline crust larger (~6.60 km/s, Figs. 9d and 10b) than for the Basin and Range, in agreement with previous studies (Table 3(a–c); e.g., Braile et al., 1982). The crust of the **Colorado Plateau** is in a region of crustal thickening that occurs over a distance of ~100 km, going from 30–35 km in the Basin and Range to >40 km (e.g., Mooney and Kaban, 2010; Zandt et al., 1995) on the plateau. The plateau remained undeformed during the Early Cenozoic compression and extension in the Rio Grande rift and Basin and Range province compared to surrounding regions (e.g., Snelson et al., 1998; van Wijk et al., 2010). The velocities estimated in the crystalline crust by previous seismic experiments (6.0 km/s–6.8 km/s) are consistent with those of rocks of silicic to intermediate composition (e.g., Snelson et al., 1998). Negative Bouguer anomalies also are indicative of low crustal density in the thickened crust of this region (Gilbert, 2012). The new model shows a gradual decrease of velocities from the eastern part close to the Rocky Mountains to the west toward the Basin and Range (Figs. 9a–d and 10a) as observed in previous studies (Snelson et al., 1998; Zandt et al., 1995) and the resulting average velocity of the crystalline crust (~6.35 km/s) is lower than the continental average (Christensen and Mooney, 1995). The model tends to underestimate the velocity in the upper crust and overestimate it in the lower crust (~ −0.20 km/s), respect to the values of the seismic data points (Table 3(a–c)). However, the three-layers' model re-interprets crustal structure of this region, since no internal discontinuity is present in the original seismic model of Snelson et al. (1998).

The **Rocky Mountains** constitute the eastern side of the broad Cordilleran orogeny that developed during late Mesozoic/early Cenozoic. Its crust is similar to the Archean craton to the east, but the existence of lower seismic velocities in the upper crust indicates that intense magmatism during the Cenozoic in the northern and southern Rocky

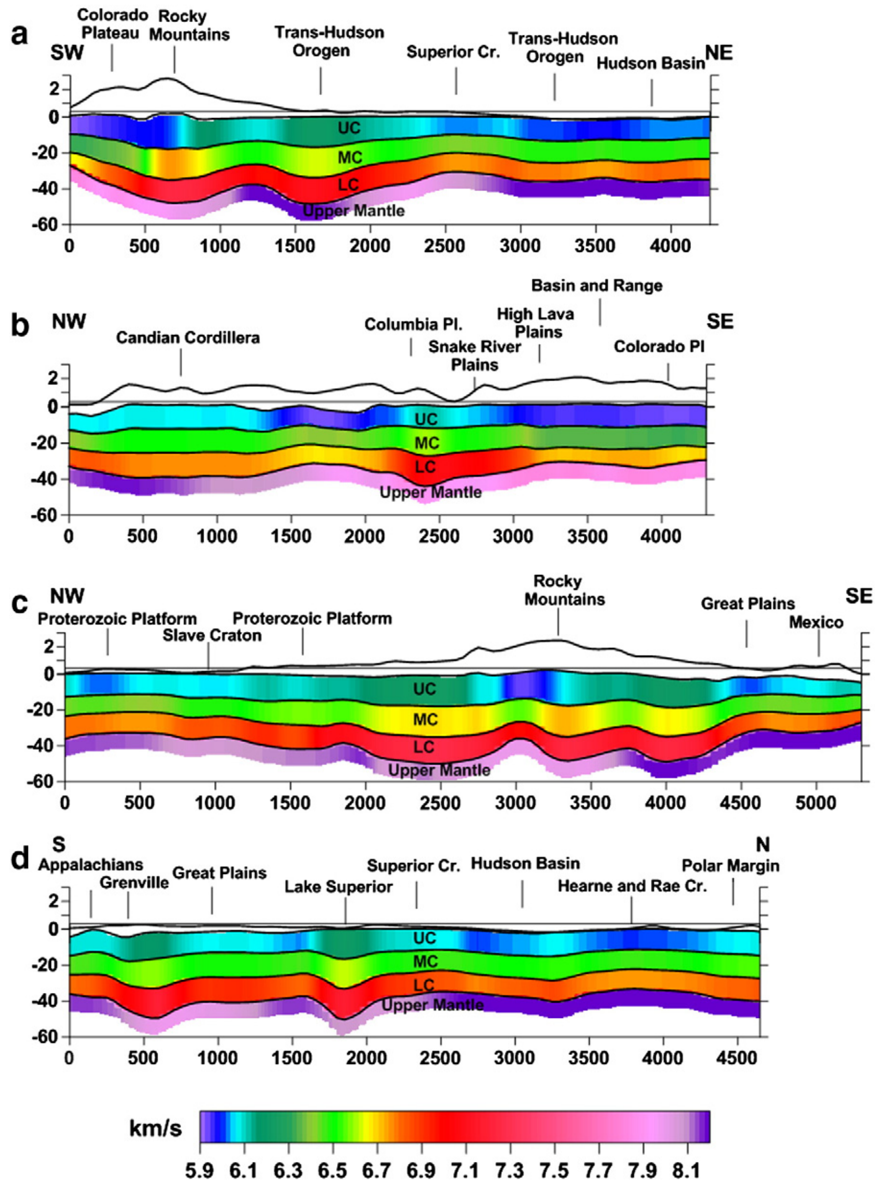

Fig. 10. (a–d) Average velocity (km/s) and thickness (km) of the upper, middle and lower crust and sub-Moho *P*-wave velocity (*Pn*) along four crustal cross-sections of the North American continent. The vertical axis of topography in respect to that of the depth of the intracrustal boundaries is ~7 times exaggerated. Cross-sections locations are displayed in Fig. 1b.

Mountains had reduced the seismic velocities in the uppermost layer and that the compression has likely thickened it, without affecting the lower crust. According to NACr14, the upper crust composes up to 40% of the entire crust and has average velocities between 5.9 and 6.2 km/s (Table 2, Figs. 9a, 10a and c), similar to those estimated in the previous studies of Snelson et al. (1998, 2004). Relatively high velocities are observed in the middle crustal layer (Snelson et al., 2004), while in the lower crust, from central Wyoming to southern Alberta, the velocity increases from 7.05 to 7.3 km/s. The '7.x layer', responsible for the deep Moho (~50 km, Mooney and Kaban, 2010) in this region, have been observed also in the 3-D Vs models of Shen et al. (2013) and Porritt et al. (in press) and appears to be a characteristic of the Archean Wyoming province. This layer, consistent with mafic garnet granulite or hornblendite compositions, similar to the compositions of xenoliths from northern Montana (Reed et al., 1993), may represent crustal thickening resulting from underplating of partially melted mafic material from the mantle (e.g., Gorman et al., 2002; Rumpfhuber and Keller, 2009; Snelson et al., 1998). The '7.x layer' is present also beneath the southern Rocky Mountains in Colorado and New Mexico, with slightly slower average velocities (Snelson et al., 2004), while north to Southern Alberta, the crust gradually thins towards the cratonic Hearne province (~40 km), where the '7.x layer' disappears. Although *Vp* and *Vs* depend on temperature and composition in a different way, we observed that, according to the study of Bensen et al. (2009), the shear waves in this region have a similar velocity distribution, with low values in the upper crust, comparable to those of tectonic provinces of western US, and anomalously high in the lower crust. The new model reproduces quite fairly the crustal structure of this tectonic province (Fig. 7a–d), displaying very large velocities of the middle (6.65–6.75 km/s) and lower crustal layer (7.15–7.25 km/s) (Fig. 10c). Respect to the values of the database, NACr14 underestimates and overestimates the velocities of the middle and lower layer, respectively (Table 3(a–c)). Such a discrepancy is related to the different depth of the intra-crustal boundaries estimated in NACr14 respect to the original seismic data points.

East to the Rocky Mountains, the **Great Plains** (central part of the midcontinent craton) is characterized by a heterogeneous crustal structure containing the '7.x layer' only along the western and southern edges of the craton (Braile et al., 1989). In order to fit the seismic data we associated a relatively large range of velocities to the crustal layers

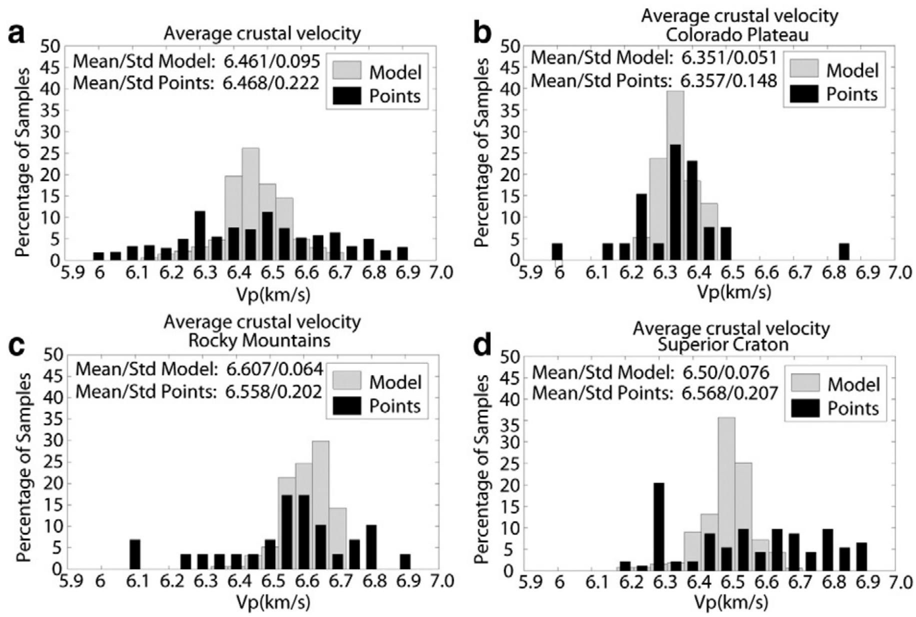

Fig. 11. (a–d) Bar plots of the average velocities (km/s) in the crystalline crust according to the model (gray bars) and of the data points (black thinner bars) for (a) the study area; (b) Colorado Plateau; (c) Rocky Mountains and (d) Superior craton. See text for further explanation.

(Table 2). The new model, in agreement with previous seismic experiments (Table 3(a–c)), shows larger thicknesses of the middle and lower crust with respect to the upper crust and high velocities of these layers (6.55 and 7.0 km/s, respectively) beneath the Mississippi embayment and the surrounding regions (Fig. 10d). There the presence of the "7.x layer" (7.3 km/s), which thickens in the north central embayment (up to 20 km), indicates that the lower crust has been altered by intrusion of mantle material during the Late Precambrian rift (Braile et al., 1989; Ginzburg et al., 1983; Mooney et al., 1983).

The **Canadian Shield** is one of the planet's largest areas of Precambrian geology (Thompson et al., 2010), comprising several Archean terranes brought together during a series of Paleoproterozoic orogenic events (Hoffman, 1988). The oldest rocks of this province (>4.0 billion years) are found in the **Slave** tectonic province, a relatively small Archean craton in northwestern Canada (Bowring et al., 1989; Stern and Bleeker, 1998). Despite the complex evolution of this region, including different phases of subduction, collision and rifting (Bleeker et al., 1999), the crust is characterized by the relatively flat Moho (35–40 km, Mooney and Kaban, 2010). The velocities of the crustal layers, according to NACr14 (Figs. 9(a–d) and 10c), show intermediate values (6.0–6.80 km/s), in agreement with the previous seismic experiments of Fernández-Viejo and Clowes (2003) (Table 3(a–c)). The resulting average velocity of the crystalline crust ~6.45 km/s (Fig. 8d), is close to that of the Earth continental crust (Christensen and Mooney, 1995).

The transition from the Archean craton to the **Paleoproterozoic platform** to the west is not marked by a change in the crustal structure (Fig. 10c). In the central part of the Wopmay orogen, developed between 2.1 Ga and 1.84 Ga (Fernández-Viejo and Clowes, 2003), by accretion of terranes and magmatic arcs, velocities in the lower crust increase up to 7.1 km s^{-1}, while velocities in the upper mantle decrease to 7.40–7.60 km/s (Fernández-Viejo and Clowes, 2003). These results have been interpreted in terms of the presence of a Palaeoproterozoic subduction zone and serpentization of the overlying mantle peridotites from fluid fluxing due to dehydration of the downgoing slab (Fernández-Viejo and Clowes, 2003). Results from previous seismic experiments in the Peace River Arch, indicate that velocities increase in the deeper part of the crust up to 7.25 km/s (Halchuk and Mereu, 1990), probably due to intrusions and underplating from the mantle. In order to fit the seismic data, we defined a small range of relative thicknesses of the upper and lower crust, instead of fixed values like for the other tectonic provinces (Table 2). The new model shows average velocities in the middle and lower crust larger than those of the neighbor Slave province, with the highest values observed beneath the Peace River Arch (Fig. 9b–c).

The **Superior craton** is a complex assemblage of continental and oceanic terranes which amalgamated in the time period ~ 3.0 to 2.6 Ga through a progression of collisional events (Darbyshire and Eaton, 2010). The velocities of the crustal layers of this tectonic province are generally high, on account of the rifting phase that occurred during the Proterozoic (~2.6 Ga) that lead to the formation of mafic volcanic rocks (e.g., Trehu et al., 1991). In the upper crust beneath Lake Superior the velocity increases up to about 6.80 km/s, on account of the basalt rocks, which have replaced part of this layer (e.g., Shay and Trehu, 1993). The high velocity lower crust (7.20–7.30 km/s), thicker beneath the axis of the central half-graben, has been interpreted as a result of the intrusion and underplating of thinned Archean crust. In order to fit the seismic data (Table 3(a–c)), we associated a large range of velocities and similar percentage of crustal thickness to the three crustal layers composing this tectonic province (Table 2). The largest velocity values in all three layers are observed beneath the Lake Superior (Figs. 9a–d and 10d), in agreement with previous studies (e.g., Musacchio et al., 2004; Shay and Trehu, 1993). The average velocity of the crystalline crust decreases from >6.65 km/s beneath the Lake Superior to <6.40 km/s in northwest direction toward the Hudson basin and in the Nain province on the Labrador margin (Figs. 9d, 10a and d), where no underplated zone has been observed (e.g., Funck and Louden, 1999; Hall and Hajnal, 1969; Musacchio et al., 2004).

The crustal structure of the **Churchill** craton is much less understood than that of the extensively studied Superior craton, due to the scarcity of seismic field measurements. The craton is divided by the Snowbird Tectonic Zone into two principal domains, the Rae to the northwest and the Hearne to the southeast. We associate a relatively low range of velocity and almost similar thickness to the three crustal layers (Table 2), composing this tectonic province, consistent with the interpretation of Németh et al. (2005) (Table 3(a–c)). The Rae craton shows lower average crustal velocities in comparison with the Hearne craton, on account of its lower crustal thickness (Figs. 1b and 10d). These results are consistent with those of the receiver functions study of Thompson et al. (2010). The latter indicate a felsic to intermediate composition (Vp/Vs ratios ~1.73) for rocks of the middle-lower crust

Table 3
Means of velocities (first three columns) and differences between the means (last two columns) for each tectonic province, estimated using the original seismic data points, NACr14 and CRUST 1.0, respectively, for upper middle and lower crust. Values are denoted by NaN when no data points are available for the corresponding crustal layer.

Upper crust					
Geological provinces	Mean (km/s) (Points)	Mean (km/s) (NACr14)	Mean (km/s) (CRUST 1.0)	Diff. (km/s) (NACr14)	Diff. (km/s) (CRUST 1.0)
Polar Margin	6.09	6.02	5.95	0.07	0.14
Slave Craton	6.08	6.06	6.20	0.02	−0.12
Paleoproterozoic	6.15	6.07	6.15	0.08	0
Churchill Craton	6.09	6.01	6.04	0.08	0.05
Trans-Hudson Orogen	6.09	6.13	6.15	−0.04	−0.06
Superior Craton	6.11	6.08	6.14	0.03	−0.03
Grenville	5.98	6.03	6.05	−0.05	−0.07
Appalachians	6.01	6.08	6.12	−0.07	−0.11
Western Mexico	5.78	6.11	5.95	−0.33	−0.17
Eastern Mexico	NaN	NaN	NaN	NaN	NaN
Gulf of Mexico	NaN	NaN	NaN	NaN	NaN
Canadian Cordillera	6.06	6.01	6.10	0.05	−0.04
Cuba	6.20	6.20	5.89	0	0.31
Great Plain	6.09	6.10	6.10	−0.01	−0.01
Rocky Mountain	6.08	6.16	6.16	−0.08	−0.08
Northern Rocky Mountain	5.96	5.98	6.07	−0.02	−0.11
Rio Grande Rift	6.04	5.96	6.02	0.08	0.02
Colorado	6.17	5.96	6.09	0.21	0.08
Basin and Range	6.00	5.96	6.11	0.04	−0.11
Southern California	5.52	5.97	6.14	−0.45	−0.62
Sierra Nevada	6.15	6.01	6.2	0.14	−0.05
Snake River Plain	6.01	6.05	6.26	−0.04	−0.25
Southern Cordillera/Columbia Plateau	5.79	5.96	6.01	−0.17	−0.22
Gulf of California	4.97	5.71	5.78	−0.74	−0.81
Southern Alaska	5.68	5.98	6.04	−0.30	−0.36
Brooks Range/NorthSlope	5.96	6.06	5.95	−0.10	0.01
Total distribution	5.99	6.05	6.08	−0.06	−0.09
Middle crust					
Geological provinces	Mean (km/s) (Points)	Mean (km/s) (NACr14)	Mean (km/s) (CRUST 1.0)	Diff. (km/s) (NACr14)	Diff. (km/s) (CRUST 1.0)
Polar Margin	NaN	NaN	NaN	NaN	NaN
Slave Craton	6.38	6.41	6.40	−0.03	−0.02
Paleoproterozoic	6.48	6.49	6.52	−0.01	−0.04
Churchill Craton	6.53	6.50	6.53	0.03	0
Trans-Hudson Orogen	6.58	6.57	6.46	0.01	0.12
Superior Craton	6.55	6.48	6.47	0.07	0.08
Grenville	6.48	6.50	6.53	−0.02	−0.05
Appalachians	6.43	6.46	6.56	−0.03	−0.13
Western Mexico	6.42	6.52	6.35	−0.10	0.07
Eastern Mexico	NaN	NaN	NaN	NaN	NaN
Gulf of Mexico	NaN	NaN	NaN	NaN	NaN
Canadian Cordillera	6.36	6.45	6.54	−0.09	−0.18
Cuba	NaN	NaN	NaN	NaN	NaN
Great Plain	6.43	6.53	6.50	−0.10	−0.07
Rocky Mountain	6.65	6.62	6.38	0.03	0.27
Northern Rocky Mountain	6.80	6.67	6.45	0.13	0.35
Rio Grande Rift	NaN	NaN	NaN	NaN	NaN
Colorado	6.37	6.32	6.30	0.05	0.07
Basin and Range	6.30	6.35	6.30	−0.05	0
Southern California	6.6	6.37	6.45	0.23	0.15
Sierra Nevada	6.65	6.39	6.30	0.26	0.35
Snake River Plain	6.52	6.52	6.54	0	−0.02
Southern Cordillera/Columbia Plateau	6.52	6.56	6.37	−0.04	0.15
Gulf of California	NaN	NaN	NaN	NaN	NaN
Southern Alaska	6.59	6.45	6.57	0.14	0.02
Brooks Range/North Slope	6.17	6.39	6.40	−0.22	−0.23
Total distribution	6.50	6.50	6.48	0	0.02
Lower crust					
Geological provinces	Mean (km/s) (Points)	Mean (km/s) (NACr14)	Mean (km/s) (CRUST 1.0)	Diff. (km/s) (NACr14)	Diff. (km/s) (CRUST 1.0)
Polar Margin	7.09	6.91	7.05	0.18	0.04
Slave Craton	6.68	6.76	6.80	−0.08	−0.12
Paleoproterozoic	6.88	6.87	6.92	0.01	−0.04
Churchill Craton	6.77	6.77	7.11	0	−0.34
Trans-Hudson Orogen	6.91	6.97	6.86	−0.06	0.05
Superior Craton	6.95	6.89	6.89	0.06	0.06
Grenville	6.84	6.87	6.93	−0.03	−0.09
Appalachians	6.85	6.82	7.06	0.03	−0.21
Western Mexico	6.88	6.83	6.85	0.05	0.03
Eastern Mexico	NaN	NaN	NaN	NaN	NaN

(continued on next page)

Table 3 (*continued*)

Lower crust					
Geological provinces	Mean (km/s) (Points)	Mean (km/s) (NACr14)	Mean (km/s) (CRUST 1.0)	Diff. (km/s) (NACr14)	Diff. (km/s) (CRUST 1.0)
Gulf of Mexico	NaN	NaN	NaN	NaN	NaN
Canadian Cordillera	6.67	6.74	7.05	−0.07	−0.38
Cuba	7.0	6.99	7.03	0.01	−0.03
Great Plain	7.01	7.03	6.9	−0.02	0.11
Rocky Mountain	6.96	7.15	6.88	−0.19	0.08
Northern Rocky Mountain	6.95	7.12	7.07	−0.17	−0.12
Rio Grande Rift	6.61	6.69	7.16	−0.08	−0.55
Colorado	6.62	6.83	6.87	−0.21	−0.25
Basin and Range	6.74	6.73	6.62	0.01	0.12
Sierra Nevada	7.12	6.84	6.8	0.28	0.32
Snake River Plain	7.04	7.04	6.97	0	0.07
Southern Cordillera/Columbia Plateau	6.85	6.81	7.02	0.04	−0.17
Gulf of California	6.55	6.58	6.98	−0.03	−0.43
Southern Alaska	6.84	6.85	7.07	−0.01	−0.23
Brooks Range/North Slope	6.96	6.81	6.95	0.15	0.01
Total distribution	6.86	6.89	6.94	−0.03	−0.08

of the Rae domain. In contrast, the Hearne craton exhibits more elevated Vp/Vs ratios (~1.76), consistent with a higher mafic component.

The Superior craton is separated from the Churchill craton by the **Trans-Hudson Orogen**, a wide zone of largely Proterozoic terranes. Velocity and thickness of the crust vary smoothly from near the Superior craton margin across the Trans-Hudson orogen to the Wyoming craton. These similarities are consistent with the hypothesis that the two cratons once formed a continuous Archean continental mass that was disrupted by the opening and closing of an oceanic basin (e.g., Stauffer, 1984). The remnants of the closing event are represented by the Trans-Hudson orogen (e.g., Green et al., 1985). In NACr14 the largest velocities of the crystalline crust of this region (~6.60 km/s, Fig. 9d), corresponding to the Moho depth >45 km (Mooney and Kaban, 2010), are related to the high lower crustal velocity (>7.0 km/s, Figs. 9c and 10a) interpreted as a segment of the trapped oceanic crust arising from the collisional environment (Németh et al., 2005). The average velocity of the crystalline crust decreases to the northwest in the Hearne craton (~6.50 km/s) and to the east in the Hudson basin (<6.40 km/s), which is mostly underlined by the Trans-Hudson orogen (e.g., Lewry and Stauffer, 1990) (Fig. 9d). Previous estimates of the average crustal velocity of the Hudson Basin (Hobson et al., 1967), which includes the contribution of the 2 km of sediments overlying the crust, predict lower values (~6.30 km/s) than NACr14 (Figs. 9d, 10a and d).

The Grenville Front, representing the orogenic boundary between the Archean Superior Province and the much younger (1.2 Ga.) **Grenville Province** to the southeast, is marked by a change in the character of the velocity gradient within the crust, as well as a significant thickening of the crust by over 5 km along the boundary zone (e.g., Mereu et al., 1986). In the southeastern Grenville province, beneath the Central Granulite Terrane, the velocities in the upper-middle crust increase due to the presence of igneous rocks related to the tectonothermal evolution of this region (Hughes and Luetgert, 1991). In contrast, velocities in the lower crust increase (up to values of 7.20 km/s) in the northwestern Grenville province (beneath the Central Metasedimentary Belt), on account of the higher mafic crustal composition. In agreement with previous seismic experiments (Table 3(a–c)), NACr14 displays such a velocity variation in the lower crust (from ~6.85 km/s to 7.0 km/s, Figs. 9a–b). According to the previous study of Prodehl et al. (1984), the largest velocities and

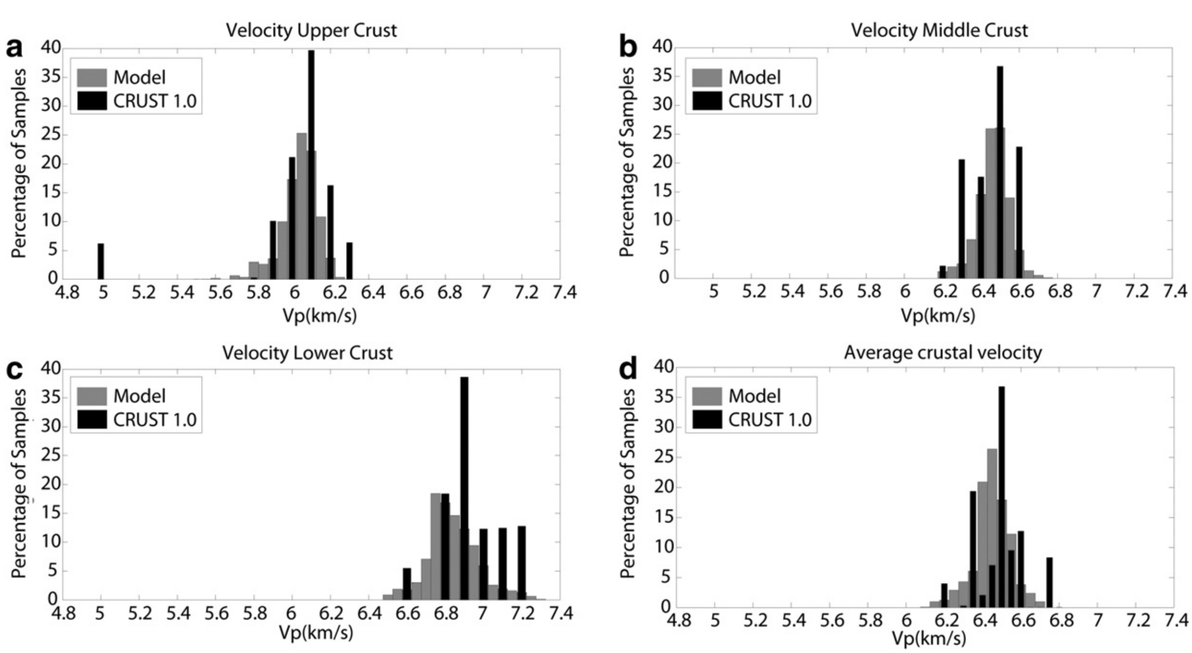

Fig. 12. (a–d) Bar plots of the average velocities (km/s) of the model (gray bars) and CRUST 1.0 (black thinner bars) in the (a) upper; (b) middle; (c) lower and (d) in the entire crystalline crust.

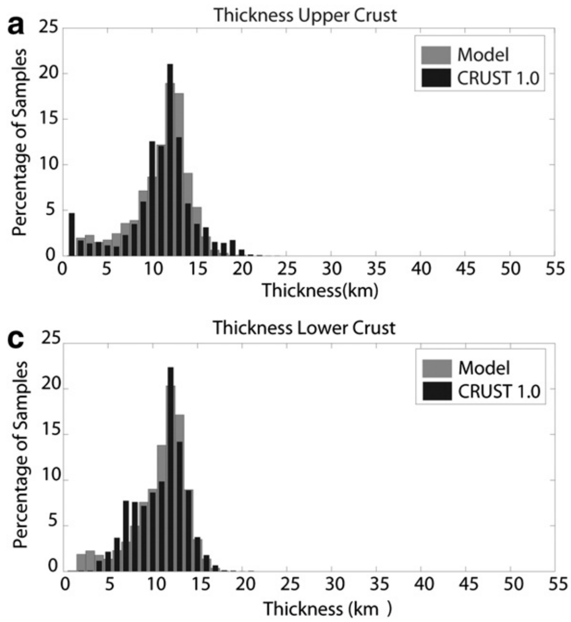

Fig. 13. (a–d) Bar plots of the thickness (km) of the (a) upper; (b) middle; (c) lower and (d) crystalline crust. Gray bars are the model and black thinner bars are CRUST 1.0.

crustal thickness (~47 km) values are estimated in the Low Plateaus in Tennessee (Figs. 9c and 10d).

The crystalline crust in the **Appalachians**, a Paleozoic orogenic belt made of accreted terranes (e.g., Hughes et al., 1994), thickens up to 45–50 km (Mooney and Kaban, 2010) and it is characterized by lower velocities respect to the Archean and Proterozoic crust. Such a velocity variation is likely related to composition, (Mareschal and Jaupart, 2004). According to previous studies (e.g., Hawman, 1996), the lower crust of the northern Appalachians is highly reflective and is characterized by high velocities (~7.0 km/s), while in the southern Appalachians it appears to be thinner and have lower velocities (6.7–6.8 km/s, Figs. 9c and 10d). Such a difference may be related to whether the arcs, accreted to form the orogenic belt, were built on oceanic or continental crust (Taylor, 1989). In both the northern and the southern Appalachians, the crust thins near the coastline with fairly low velocities occurring in the lower crust. The new model, showing relatively small ranges of velocities of the crustal layers having similar thickness (Table 2, Figs. 9d and 10d), is in agreement with the values of the database (Table 3(a–c)). The latter are consistent with rocks of intermediate composition (Hughes et al., 1994; Marillier et al., 1994).

The ranges of velocities and percentage of thickness that we associated to the crustal layers of **Mexico** are very similar to those estimated for the neighbor tectonic province of the southern Appalachians (Table 2). Actually, on account of the lack of seismic constraints in Mexico, we prefer to introduce a smooth change of the velocity and thickness of the crustal layers in this region, with respect to the neighboring tectonic province.

The crustal thickness of the **Gulf of Mexico** shows an unusual variation, from the typical oceanic thickness of about 5 km up to >15 km under the shelf. The crustal velocity, tending to increase toward the center of the basin, also shows considerable lateral variations, suggesting a non-uniform extension of the continental margin at the time of the formation of the Gulf basin (Ebeniro et al., 1988). In this region the crystalline crust does not show any intracrustal boundary and the velocity inferred corresponds to that of a basaltic rock (Table 2).

The island of **Cuba**, adjacent to the Antilles island arc, is located in the southern margin of the North America plate in direct contact with the Caribbean plate. The crust of this region is thin (<30 km, Mooney and Kaban, 2010) and is interpreted as the final result of the first period of tectonic activity (Jurassic–Middle Eocene), during which an island arc with continental crust was formed on oceanic basement (Pushcharovskiy, 1979), and the second period (Late Eocene–Quaternary), when these terranes, as a whole, were subjected to several deformation phases (Toiran, 2003). The new crustal model, according to the receiver functions study of Toiran (2003) (Table 3(a–c)), displays only two layers having relatively high velocities (6.20 km/s and 7.0 km/s, respectively, Fig. 9c).

7. Crustal parameters variability

In this section we discuss the statistical analysis of the crustal structure of NACr14 in comparison with that of the global model CRUST 1.0 (Laske et al., 2013) and other previous models. Bar plots of the crustal velocities, boundaries and thickness of the main layers of the new crustal model and CRUST 1.0 are shown in Figs. 12(a–d) and 13 (a–d).

The velocity in the upper crust spans in a relatively narrow range (Fig. 12a), with more than 75% of the values between 6.0 and 6.1 km/s and reaching a maximum value of 6.25 km/s. In respect to CRUST 1.0 the velocities of NACr14, having a similar mean, but a lower standard deviation (std; Table 4), are more uniformly distributed in the whole range, showing a larger spatial variability. The velocity in the middle crust spans between 6.20 km/s and 6.78 km/s, with more

Table 4
Comparison of the statistical analysis of the crustal parameters for NACr14 and CRUST 1.0 (North America).

Models	Velocity (km/s) Upper crust	Velocity (km/s) Middle crust	Velocity (km/s) Lower crust	Thickness (km) Upper crust	Thickness (km) Middle crust	Thickness (km) Lower crust
NACr14	6.04/0.09	6.46/0.08	6.84/0.13	11.04/3.15	11.09/3.07	10.86/3.00
CRUST1.0	6.02/0.28	6.46/0.11	6.94/0.15	10.96/2.75	11.84/3.52	10.90/3.91

Table 5
Comparison of the statistical analysis of the seismic average velocity and crustal thickness of the crystalline crust of this study (North America) and previous global and regional models.

Models	Velocity (km/s) Crystalline crust	Thickness (km/s) Crystalline crust	Pn (km/s)
CRUST1.0 Laske et al. (2013) (North America)	6.501/0.111	33.61/8.96	–
CRUST1.0 Laske et al. (2013) (North America) (Including off-shore regions)	6.490/0.123	32.59/9.78	–
Christensen and Mooney (1995) (global)	6.45/0.23	–	8.07
NACr14 (North America)	6.446/0.095	32.85/9.05	8.098
NACr14 (North America) (Including off-shore regions)	6.450/0.094	31.82/9.85	8.10
Chulick and Mooney, 2002 (North America)	6.456/0.244	–	8.041
Braile et al., 1989 (U.S. and Southern Canada)	6.435/0.235	–	8.018
Chulick et al., 2013 (South America)	6.467/0.245	–	7.998
Chulick et al., 2013 (South America) (Including off-shore regions)	6.580/0.280	–	8.013

than 80% of values distributed around two peaks of 6.4 km/s and 6.5 km/s (Fig. 12b). In contrast, in CRUST 1.0 the values have a mean and std similar to our model, but are distributed only around four main peaks (Table 4). The average velocity in the lower crust ranges from 6.45 km/s to 7.28 km/s, with ~90% of values between 6.7 km/s and 7.0 km/s. In CRUST 1.0, the average velocities of this layer span from 6.6 km/s to 7.2 km/s, but also in this case the values are not uniformly distributed (Fig. 12c). More than 70% of values are over 6.80 km/s, which results in a larger mean with respect to NACr14 (Table 4). In general, the smaller variance and the more nearly Gaussian distribution of the velocities of our new model may be due to the method used and does not necessarily provide evidence for higher reliability. However, the lower spatial variability of the velocities shown by the histograms of CRUST 1.0 reflects the fact that wide tectonic provinces are characterized by a single value (Laske et al., 2013). This approach gives unrealistically uniform velocity distribution within each tectonic province and sharp velocity contrasts across their borders. In contrast, our method, which estimates velocity variations within a number of tectonic provinces on the basis of the trends shown by the seismic data, gives more realistic interpretations of the crustal seismic velocity structure.

The values of the average velocity of the crystalline crust in NACr14 (Fig. 12d) range from 6.1 km/s to 6.7 km/s with the mean value for the on-shore part of the North American continent (6.45 km/s), larger than that estimated by Braile et al. (1989) and slightly lower than those estimated by Christensen and Mooney (1995) for the world. These values are also slightly lower than estimates by Chulick and Mooney (2002) for North America and by Chulick et al. (2013) for South America (Table 5). The largest values are found mostly in the regions characterized by a high velocity lower crust, while the lowest values correspond to the regions of recent crustal extension having relatively high heat flow (e.g., Basin and Range). Including the off-shore regions, the mean value (6.45 km/s) slightly increases, due to the oceanic crustal type characterizing the Gulf of Mexico. The average velocities of the crystalline crust, provided by CRUST 1.0 are not uniformly distributed and show a larger mean value, related to the larger average value of the lower crust (Table 5). In particular, the average of the whole crustal velocity in the Canadian Cordillera is larger (~6.55 km/s) than other neighboring tectonic provinces.

The thicknesses of each of the three crustal layers usually represent 30%–40% of the entire crystalline crust (Figs. 13(a–c)), spanning in a range between 2 and 18 km, with more than 50% of the values concentrated between 11 km and 13 km. The layers have similar mean and std (~11.0 km and ~3.0 km, respectively) (Table 4). CRUST 1.0 shows similar values, with the main peaks of the thickness of the middle crust shifted respect to NACr14 to slightly larger values (Fig. 13b). However, the geographical distribution of the values of CRUST 1.0 differs significantly from those of NACr14. For instance, the thicknesses of the lower crust estimated by CRUST 1.0 are remarkably lower (~6 km) than those of our model (11–16 km, Fig. 9c) in most of the North American Cordillera. The thickness of the crystalline crust of our model is continuously distributed in a range between 4 and 51 km, with the lowest values corresponding to the off-shore regions. In contrast, CRUST 1.0 spans in a larger range between 3 and 57 km with a mean peak around 37 km and a mean value slightly higher compared to our model (Fig. 13d).

8. Conclusions

We have constructed NACr14, a 3D model of the crystalline crust of the North American continent, providing estimates for the thickness, average velocities of the main crustal layers and the *Pn* velocity. The basis for our study is a detailed compilation of crustal seismic models in this region (USGS database). However, on account of the uneven distribution of the seismic data, we could not directly interpolate the values of the crustal parameters. Hence, we selected and analyzed the seismic data composing the USGS database and we estimated the *P-wave* seismic velocity and thickness of the upper, middle and lower crust for each pre-defined tectonic province. At the same time, the relatively larger number of seismic profiles providing *Pn* data makes it possible the direct interpolation of the values of this parameter on a uniform grid.

The seismic velocities with the crystalline crust of this new model with a resolution of 1° × 1° are quite consistent with those of the measured seismic data. The differences found are related to: (1) the unequal distribution of the data points; (2) the possible presence of outliers between the data points; (3) the existence of strong crustal heterogeneities not reproduced by NACr14. The main variations of the crustal structure reflect the tectonic evolution of the tectonic provinces. Velocities of the lower crust vary in a larger range than those of the other layers, while the thickness of all the three layers is on average between 11 and 13 km. The largest velocities of the crystalline crust (>6.6 km/s) reflect the presence of a 7.x layer (>7.0 km/s) in the lowermost part of the crust. In comparison with CRUST 1.0, NACr14 is more heterogeneous, showing a larger spatial variability of the thickness and average velocities of the crustal layers.

The digital model with a resolution of 1° × 1° degree is available in the supplementary materials and can be used in many geophysical applications.

Acknowledgements

This study was funded by an Alexander von Humboldt Foundation post-doctoral grant and award, GeoForschungsZentrum, Potsdam, the USGS National Earthquake Hazards Reduction Program and the Netherlands Research Centre for Integrated Solid Earth (ISES). We are grateful to two anonymous reviewers for the constructive reviews of this paper.

Appendix A. Supplementary data

Supplementary data to this article can be found online at http://dx.doi.org/10.1016/j.tecto.2014.04.016.

References

Artemieva, I.M., Thybo, H., 2013. Moho discontinuity and crustal structure in Europe, Greenland, and the North Atlantic region. Tectonophysics 609, 97–153.

Bassin, C., Laske, G., Masters, G., 2000. The current limits of resolution for surface wave tomography in North America. Eos 81, F897.

Becker, T.W., Faccenna, C., 2011. Mantle conveyor beneath the Thetyan collisional belt. Earth Planet. Sci. Lett. 310, 453–461.

Bedle, H., van der Lee, S., 2009. S velocity variations beneath North America. J. Geophys. Res. 114, B07308. http://dx.doi.org/10.1029/2008JB005949.

Bensen, G.D., Ritzwoller, M.H., Yang, Y., 2009. A 3-D shear velocity model of the crust and uppermost mantle beneath the United States from ambient seismic noise. Geophys. J. Int. 177, 1177–1196.

Berry, M.J., Fuchs, K., 1973. Crustal structure of the superior and Grenville provinces of the Northeastern Canadian Shield. Bull. Seismol. Soc. Am. 63 (4), 1393–1432.

Blackwell, D.D., Richards, M., 2004. Geothermal map of North America, scale 1:6,500,000, 1 sheet, Am. Assoc. of Petroleum Geol., Tulsa, Okla.

Blackwell, D., Steele, J., Carter, L., 1991. Heat-flow patterns of the North American continent: a discussion of the geothermal map of North America. In: Slemmons, D., et al. (Eds.), Decade of North American Geology. Geol. Soc. of Am., vol. 1. Neotectonics of North America, Boulder, Colorado.

Bleeker, W., Ketchum, J.W.F., Jackson, V.A., Villeneuve, M.E., 1999. The central Slave basement complex, part I: Its structural topology and autochthonous cover. Can. J. Earth Sci. 36, 1083–1109.

Boschi, L., Faccenna, C., Becker, T.W., 2010. Mantle structure and dynamic topography in the Mediterranean Basin. Geophys. Res. Lett. 37, L20303. http://dx.doi.org/10.1029/2010GL045001.

Bouligand, C., Glen, J.M.G., Blakely, R.J., 2009. Mapping Curie temperature depth in the western United States with a fractal model for crustal magnetization. J. Geophys. Res. 114, B11104. http://dx.doi.org/10.1029/2009JB006494.

Bowring, S.A., Williams, I.S., Compston, W., 1989. 3.96 Ga gneisses from the Slave Province. Geology 17, 971–975.

Braile, L.W., Smith, R.B., Ansorge, J., Baker, M.R., Sparlin, M.A., Prodehl, C., Schilly, M.M., Healy, J.H., Mueller, St, Olsen, K.H., 1982. The Yellowstone-Snake River Plain seismic profiling experiment: crustal structure of the eastern Snake River Plain. J. Geophys. Res. 87 (B4), 2597–2609.

Braile, L.W., Hinze, W.J., von Frese, R.R.B., Keller, G.R., 1989. Seismic properties of the crust and uppermost mantle of the conterminous United States and adjacent Canada. In: Pakiser, L.C., Mooney, W.D. (Eds.), Geophysical Framework of the Continental United States. Geol. Soc. Am. Memoir, 172, pp. 655–680.

Buehler, J.S., Shearer, P.M., 2012. Localized imaging of the uppermost mantle with USArray *Pn* data. J. Geophys. Res. 117, B09305. http://dx.doi.org/10.1029/2012JB009433.

Catchings, R.D., 1992. A relation among geology, tectonics, and velocity structure, western to central Nevada Basin and Range. Geol. Soc. Am. Bull. 104, 1178–1192.

Catchings, R.D., Mooney, W.D., 1988a. Crustal structure of the Columbia plateau: evidence for continental rifting. J. Geophys. Res. 93 (B1), 459–474.

Catchings, R.D., Mooney, W.D., 1988b. Crustal structure of east central Oregon: relation between Newberry Volcano and regional crustal structure. J. Geophys. Res. 93 (B9), 10081–10094.

Catchings, R.D., Mooney, W.D., 1991. Basin and Range crustal and upper mantle structure, northwest to central Nevada. J. Geophys. Res. 96 (4), 6247–6467.

Christensen, N.I., Mooney, W.D., 1995. Seismic velocity structure and composition of the continental crust: a global review. J. Geophys. Res. 100, 9761–9788.

Chulick, G.S., Mooney, W.D., 2002. Crustal structure of North America and adjacent oceanic basins: a synthesis. Bull. Seismol. Soc. Am. 92, 2478–2492.

Chulick, G.S., Detweiler, S., Mooney, W.D., 2013. Seismic structure of the crust and uppermost mantle of South America and surrounding oceanic basins. J. S. Am. Earth Sci. 42, 260–276.

Clowes, R.M., Hammer, P.T.C., Fernández-Viejo, G., Welford, J.K., 2005. Lithospheric structure in northwestern Canada from Lithoprobe seismic refraction and related studies: a synthesis. Can. J. Earth Sci. 42, 1277–1293.

Colburn, R.H., Mooney, W.D., 1986. Two-dimensional velocity structure along the synclinal axis of the Great Valley. Calif. Bull. Seismol. Soc. Am. 76, 1305–1322.

Colgan, J., Dumitru, T., Miller, E., Reiners, P., 2006. Cenozoic tectonic evolution of the Basin and Range Province in northwestern Nevada. Am. J. Sci. 306, 616–654.

Creaser, B., Spence, G., 2005. Crustal structure across the northern Cordillera, Yukon Territory, from seismic wide-angle studies: Omineca Belt to Intermontane Belt. Can. J. Earth Sci. 42, 1187–1203.

Darbyshire, F.A., Eaton, D.W., 2010. The lithospheric root beneath Hudson Bay, Canada from Rayleigh wave dispersion: no clear seismological distinction between Archean and Proterozoic mantle. Lithos 120, 144–159.

Eagar, K.C., Fouch, M.J., James, D.E., Carlson, R.W., 2011. Crustal structure beneath the High Lava Plains of eastern Oregon and surrounding regions from receiver function analysis. J. Geophys. Res. 116, B02313. http://dx.doi.org/10.1029/2010JB007795.

Eaton, J.P., 1966. Crustal structure in northern and central California from seismic evidence. Geology of Northern California. Cal. Div. Mines Geology Bull., 190, p. 419.

Ebeniro, J.O., Nakamura, Y., Sawyer, D.S., O'Brien, W.P., 1988. Sedimentary and crustal structure of the northwestern Gulf of Mexico. J. Geophys. Res. 93 (B8), 9075–9092.

Ellis, R.M., Hajnal, Z., Bostock, M.G., 1996. Seismic studies on the Trans-Hudson Orogen of western Canada. Tectonophysics 262, 35–50.

Fernández-Viejo, G., Clowes, R.M., 2003. Lithospheric structure beneath the Archaean Slave Province and Proterozoic Wopmay orogen, northwestern Canada, from a LITHOPROBE refraction/wide-angle reflection survey. Geophys. J. Int. 153, 1–19.

Fuis, G.S., Ambos, E.L., Mooney, W.D., Christensen, N.I., 1991. Crustal structure of accreted terranes in southern Alaska, Chugach Mountains and Copper River Basin, flow seismic refraction results. J. Geophys. Res. 96 (B3), 4187–4227.

Funck, T., Louden, K.E., 1999. Wide-angle seismic transect across the Torngat Orogen northern Labrador: evidence for a Proterozoic crustal Root. J. Geophys. Res. 104, 7463–7480.

Gilbert, H., 2012. Crustal structure and signatures of recent tectonism as influenced by ancient terranes in the western United States. Geosphere 8 (1), 141–157.

Ginzburg, A., Mooney, W.D., Walter, A.W., Lutter, W.J., Healy, J.H., 1983. Deep structure of northern Mississippi Embayment. Am. Assoc. Pet. Geol. Bull. 67 (11), 2031–2046.

Gorman, A.R., Clowes, R.M., Ellis, R.M., Henstock, T.J., Spence, G.D., Randy Keller, G., Levander, A., Snelson, C.M., Burianyk, M.J.A., Ernest Kanasewich, R., Asudeh, I., Hajnal, Z., Miller, K.C., 2002. Deep probe: imaging the roots of western North America. Can. J. Earth Sci. 39, 375–398.

Green, A.G., Hajnal, Z., Weber, W., 1985. An evolutionary model of the western Churchill province and western margin of the Superior province in Canada and the north-central United States. Tectonophysics 16, 281–322.

Hajnal, Z., 1992. Nature of the Canadian polar margin northwest of Axel Heiberg Island. Tectonophysics 201, 255–275.

Halchuk, S.C., Mereu, R.F., 1990. A seismic investigation of the crust and Moho underlying the Peace River Arch, Canada. Tectonophysics 185, 1–19.

Hall, D.H., Hajnal, Z., 1969. Crustal structure of northwestern Ontario, refraction seismology. Can. J. Earth Sci. 6, 81–99.

Hammer, P.T.C., Clowes, R.M., 2004. Accreted terranes of northwestern British Columbia, Canada: lithospheric velocity structure and tectonics. J. Geophys. Res. 109, B06305. http://dx.doi.org/10.1029/2003JB002749.

Hardebol, N.J., Beekman, F., Cloetingh, S.A.P.L., 2013. Strong lateral strength contrasts in the mantle lithosphere of continents: a case study from the hot SW Canadian Cordillera. Tectonophysics 602, 87–105.

Hawman, R., 1996. Wide-angle, three component seismic reflection profiling of the crust along the East Coast Gravity High, southern Appalachians, using quarry blasts. J. Geophys. Res. 101, 15867.

Hobson, G.D., Overton, A., Clay, D.N., Thatcher, W., 1967. Crustal structure under Hudson Bay. Can. J. Earth Sci. 45, 929–947.

Hoffman, P., 1988. United plates of America, the birth of a craton: early Proterozoic assembly and growth of Laurentia. Ann. Rev. Earth Planet. Sci. 16, 543–603.

Holbrook, W.S., Mooney, W.D., 1987. The crustal structure of the axis of the Great Valley, California, from seismic refraction measurements. Tectonophysics 140, 49–63.

Hughes, S., Luetgert, J., 1991. Crustal Structure of the Western New England Appalachians and the Adirondack Mountains. J. Geophys. Res. 96 (B10), 16,471–16,494.

Hughes, S., Hall, J., Luetgert, J.H., 1994. The seismic velocity structure of the Newfoundland Appalachian orogen. J. Geophys. Res. 99 (B7), 13663.

Kaban, M.K., Tesauro, M., Cloetingh, S.A.P.L., 2010. An integrated gravity model for Europe's crust and upper mantle. Earth Planet. Sci. Lett. 296, 195–209.

Kanasewich, E.R., Burianyk, M.J.A., Ellis, R.M., Clowes, R.M., White, D.J., Côté, T., Forsyth, D. A., Luetgert, J.H., Spence, G.D., 1994. Crustal velocity structure of the Omineca Belt, southeastern Canadian Cordillera. J. Geophys. Res. 99 (B2), 2653–2670.

Koulakov, I., Kaban, M.K., Tesauro, M., Cloetingh, S., 2009. P- and S-velocity anomalies in the upper mantle beneath Europe from tomographic inversion of ISC data. Geophys. J. Int. 179, 345–366.

Laske, G., Masters, G., Ma, Z., Pasyanos, M., 2013. Update on CRUST1.0 — a 1-degree global model of Earth's crust. Geophys. Res. Abstr. 15 (Abstract EGU2013-2658, 2013).

Lerch, D.W., Klemperer, S.L., Glen, J.M.G., Ponce, D.A., Miller, E.L., Colgan, J.P., 2007. Crustal structure of the northwestern Basin and Range Province and its transition to unextended volcanic plateaus. Geochem. Geophys. Geosyst. 8 (2), Q02011. http://dx.doi.org/10.1029/2006GC001429.

Levander, A., Miller, M.S., 2012. Evolutionary aspects of lithosphere discontinuity structure in the western U.S. Geochem. Geophys. Geosyst. 13 (1), Q0AK07. http://dx.doi.org/10.1029/2012GC004056.

Lewis, T.J., Hyndman, R.D., Flück, P., 2003. Heat flow, heat generation, and crustal temperatures in the northern Canadian Cordillera: thermal control of tectonics. J. Geophys. Res. 108 (B6), 2316. http://dx.doi.org/10.1029/2002JB002090.

Lewry, J.F., Stauffer, M.R. (Eds.), 1990. The Early Proterozoic Trans-Hudson Orogen of North America: Geological Association of Canada Special Paper, 37 (505 pp.).

Mahan, K.H., Schulte-Pelkum, V., Shen, W., Ritzwoller, M.H., 2012. Seismic and petrological constraints on deep crustal evolution in North America: where and what are 7.x layers? AGU Fall Meeting, San Francisco, CA, USA (Presentation).

Majdański, M., 2013. The uncertainty in layered models from wide-angle seismic data. Geophysics 78, 3.

Mareschal, J.C., Jaupart, C., 2004. Variations of surface heat flow and lithospheric thermal structure beneath the North American craton. Earth Planet. Sci. Lett. 223, 65–77.

Marillier, F., Hall, J., Hughes, S., Louden, K., Reid, I., Roberts, B., Clowes, R., Coté, T., Fowler, J., Guest, S., Lu, H., Luetgert, J., Quinlan, G., Spencer, C., Wright, J., 1994. Lithoprobe East onshore-offshore seismic refraction survey-constraints on interpretation of reflection data in the Newfoundland Appalachians. Tectonophysics 232, 43–58.

Meqbel, N.M., Egbert, G.D., Wannamaker, P.E., Kelbert, A., Schultz, A., 2014. Deep electrical resistivity structure of the northwestern U.S. derived from 3-D inversion of USArray magnetotelluric data. Earth Planet. Sci. Lett. (in press).

Mereu, R., Wang, D., Kuhn, O., 1986. Evidence for an inactive rift in the Precambrian from a wide-angle reflection survey across the Ottawa–Bonnechere graben. In: Barazangi, M., Brown, L.D. (Eds.), Reflection Seismology: The Continental Crust. Geodyn. Ser., 14. AGU, Washington, D.C, pp. 127–134.

Molinari, I., Morelli, A., 2011. EPcrust: a reference crustal model for the European Plate. Geophys. J. Int. 185, 352–364.

Mooney, W.D., 2014. Global crustal structure, In: Romanowicz, B., Dziewonski, A. (Eds.), Second Edition. Crust and Mantle, vol. 1. Elsevier, Netherlands (volume editors, G. Schubert, Treatise editor-in-Chief, in press).

Mooney, W.D., Braile, L.W., 1989. The seismic structure of the continental crust and upper mantle of North America. In: Bally, A.W., Palmer, A.R. (Eds.), The Geology of North America: An Overview. Geological Society of America, Boulder, Colorado, pp. 39–52.

Mooney, W.D., Kaban, M.K., 2010. The North American upper mantle: density, composition, and evolution. J. Geophys. Res. 115, B12424. http://dx.doi.org/10.1029/2010JB000866.

Mooney, W.D., Andrews, M.C., Ginzburg, A., Peters, D.A., Hamilton, R.M., 1983. Crustal structure of the northern Mississippi embayment and a comparison with other continental rift zones. Tectonophysics 94, 327–348.

Mooney, W.D., Laske, G., Masters, G., 1998. CRUST 5.1: a global crustal model of 5 × 5. J. Geophys. Res. 103, 727–747.

Moore, T.E., Wallace, W.K., Bird, K.J., Karl, S.M., Mull, C.G., Dillon, J.T., 1994. Geology of northern Alaska. In: Plafker, G., Berg, H.C. (Eds.), The Geology of North America. Geol. Soc. of Am., vol. G-l. The Geology of Alaska, Boulder, Colo, pp. 49–140.

Musacchio, G., White, D.J., Asudeh, I., Thomson, C.J., 2004. Lithospheric structure and composition of the Archean western Superior Province from seismic refraction/wide angle reflection and gravity modeling. J. Geophys. Res. 109, B03304. http://dx.doi.org/10.1029/2003JB002427.

Németh, B., Clowes, R.M., Hajnal, Z., 2005. Lithospheric structure of the Trans-Hudson Orogen from seismic refraction — wide-angle reflection studies. Can. J. Earth Sci. 42, 435–456.

Pakiser, L.C., Steinhart, J.S., 1964. Explosion seismology in the western hemisphere. In: Odishaw, J. (Ed.), Research in Geophysics: Solid Earth and Interface Phenomena, 2. Massachusetts Institute of Technology Press, Cambridge, pp. 123–147.

Patro, P.K., Egbert, G.D., 2008. Regional conductivity structure of Cascadia: preliminary results from 3D inversion of USArray transportable array magnetotelluric data. Geophys. Res. Lett. 35, L20311. http://dx.doi.org/10.1029/2008GL035326.

Phillips, R.P., 1964. Seismic refraction studies in Gulf of California. In: Van Andel, T.H., Shor Jr., G.G. (Eds.), Marine Geology of the Gulf of California. Am. Assoc. Petr. Geol., Mem., 3, p. 90.

Porritt, R.W., Allen, R.M., Pollitz, F.F., 2014. Seismic imaging east of the Rocky Mountains with USArray. Earth Planet. Sci. Lett. (in press).

Prodehl, C., Mooney, W.D., 2012. Exploring the Earth's crust: history and results of controlled-source seismology. Mem. Geol. Soc. Am. 208 (764 pp.).

Prodehl, C., Schlittenhardt, J., Stewart, J.W., 1984. Crustal structure of the Appalachian Highlands in Tennessee. Tectonophysics 109 (1–2), 61–76.

Pushcharovskiy, Y.M., 1979. The tectonics and geodynamics of the Caribbean region. Tektonicheskoye razvitiye zemnoy kory I razlomy (Tectonic Evolution of the Earth's Crust and Faults)Nauka, Moscow pp. 124–132.

Reed Jr., J.C., Ball, T.T., Farmer, G.L., Hamilton, W.B., 1993. In: Reed Jr., J.C., et al. (Eds.), A broader view. Precambrian: Conterminous, C-2. Geological Society of America, Geology of North, America, U.S.: Boulder, Colorado, pp. 597–636.

Rumpfhuber, E.M., Keller, R.G., 2009. An integrated analysis of controlled and passive source seismic data across an Archean-Proterozoic suture zone in the Rocky Mountains. J. Geophys. Res. 114, B08305. http://dx.doi.org/10.1029/2008JB005886.

Schmandt, B., Humphreys, E., 2011. Seismically imaged relict slab from the 55 Ma Siletzia accretion to the northwest United States. Geology 39, 175–178. http://dx.doi.org/10.1130/G31558.1.

Shay, J., Trehu, A., 1993. Crustal structure of the central graben of the Midcontinent Rift beneath Lake Superior. Tectonophysics 225, 301–335.

Shen, W., Ritzwoller, M.H., Schulte-Pelkum, V., 2013. A 3-D model of the crust and uppermost mantle beneath the Central and Western US by joint inversion of receiver functions and surface wave dispersion. J. Geophys. Res. 118, 1–15.

Sinno, Y.A., Daggett, P.H., Keller, G.R., Morgan, P., Harder, S.H., 1986. Crustal structure of the Southern Rio Grande Rift determined from seismic refraction profiling. J. Geophys. Res. 91, 6143–6156.

Smith, R.B., Schilly, M.M., Braile, L.W., Ansorge, J., Lehman, J.L., Baker, M.R., Prodehl, C., Healy, J.H., Mueller, S., Greensfelder, R.W., 1982. The 1978 Yellowstone-eastern Snake River plain seismic profiling experiment, crustal structure of the Yellowstone region and experimental design. J. Geophys. Res. 87 (B4), 2583–2596.

Smith, R.B., Nagy, W.G., Julander, K.A., Viveiros, J.J., Barker, C.A., Gants, D.G., 1989. Geophysical and tectonic framework of the eastern Basin and Range–Colorado Plateau–Rocky Mountain transition. In: Pakiser, L.C., Mooney, W.D. (Eds.), Geophysical Framework of the Continental United States. Geol. Soc. Am. Memoir, 172, pp. 655–680.

Smith, D., Gans, P., Miller, E., 1991. Palinspastic restoration of Cenozoic extension in the central and eastern Basin and Range Province at latitude 39–40N. In: Raines, G., et al. (Eds.), Geology and Ore Deposits of the Great Basin. Geol. Soc. of Nev, Reno, pp. 75–86.

Snelson, C.M., Henstock, T.J., Keller, G.R., Miller, K.C., Levander, A., 1998. Crustal and uppermost mantle structure along the Deep Probe seismic profile. Rocky Mt. Geol. 33 (2), 181–198.

Snelson, C.M., Keller, G.R., Miller, K.C., Rumpel, H.M., Prodehl, C., 2004. Regional crustal structure derived from the CD-ROM 99 seismic refraction/wide angle reflection profile: the lower crust and upper mantle. Copyright 2004 by the American Geophysical Union 10.1029/Series#LettersChapter#.

Sparlin, M.A., Braile, L.W., Smith, R.B., 1982. Crustal structure of the eastern Snake River plain determined from ray trace modeling of seismic refraction data. J. Geophys. Res. 87 (B4), 2619–2633.

Stauber, D.A., Boore, D.M., 1978. Crustal thickness in Northern Nevada from seismic refraction profiles. Bull. Seismol. Soc. Am. 68 (4), 1049–1058.

Stauffer, M.R., 1984. Manikewan: an early Proterozoic ocean in central Canada, its igneous history and orogenic closure. Precambrian Res. 25, 257–281.

Stern, R.A., Bleeker, W., 1998. Age of the world's oldest rocks refined using Canada's SHRIMP: the Acasta Gneiss Complex, Northwest Territories, Canada. Geosci. Can. 25, 27–31.

Steward J.H., Carlson J.E., 1976. Cenozoic rocks of Nevada: Nevada Bureau of Mines and Geology Map 52, scale 1:1,000,000.

Stolk, W., Kaban, M.K., Beekman, F., Tesauro, M., Mooney, W.D., Cloetingh, S., 2014. High resolution regional crustal models from irregularly distributed data: application to Asia and adjacent areas. Tectonophysics 602, 55–68.

Swanberg, C.A., 1979. Chemistry of the thermal and non-thermal groundwater in the Rio Grande rift and adjacent tectonic provinces. In: Riecker, R.E. (Ed.), Rio Grande Rift: Tectonics and Magmatism. AGU, Washington, D.C, pp. 279–288.

Sweeney, J.F., 1985. Comments about the age of the Canada basin. Tectonophysics 114, 1–10.

Taylor, S.R., 1989. Geophysical framework of the Appalachians and adjacent Grenville Province. In: Pakiser, L.C., Mooney, W.D. (Eds.), Geophysical Framework of the Continental United States. Geol. Soc. Am. Memoir, 172, pp. 655–680.

Tesauro, M., Kaban, M.K., Cloetingh, S.A.P.L., 2008. EuCRUST-07: a new reference model for the European crust. Geophys. Res. Lett. 35, L05313.

Tesauro, M., Kaban, M.K., Cloetingh, S.A.P.L., 2009. A new thermal and rheological model of the European lithosphere. Tectonophysics 476, 478–495.

Tesauro, M., Burov, E., Kaban, M.K., Cloetingh, S.A.P.L., 2011. Ductile crustal flow in Europe's lithosphere. Earth Planet. Sci. Lett. 312, 254–265.

Tesauro, M., Kaban, M.K., Cloetingh, S.A.P.L., 2012. Global strength and elastic thickness of the lithosphere. Glob. Planet. Chang. 90–91, 51–57.

Thompson, D.A., Bastow, I.D., Helffrich, G., Kendall, J.-M., Wookey, J., Snyder, D.B., Eaton, D. W., 2010. Precambrian crustal evolution: seismic constraints from the Canadian Shield. Earth Planet. Sci. Lett. 297, 655–666.

Toiran, B.M., 2003. The crustal structure of Cuba derived from Receiver Function Analysis. J. Seism. 7, 359–375.

Trehu, A., Morel a l' Huissier, P., Meyer, R., Hajnal, Z., Karl, J., Mereu, R., Sexton, J., Shay, J., Chan, W.K., Epili, D., Jefferson, T., Shih, X.R., Wendling, S., Mikereit, B., Green, A., Hutchinson, D., 1991. Imaging the Midcontinent Rift beneath Lake Superior using large aperture seismic data. Geophys. Res. Lett. 18 (4), 625–628.

van Wijk, J.W., Baldridge, W.S., van Hunen, J., Goes, S., Aster, R., Coblentz, D.D., Grand, S.P., Ni, J., 2010. Small-scale convection at the edge of the Colorado Plateau: implications for topography, magmatism, and evolution of Proterozoic lithosphere. Geology 38 (7), 611–614. http://dx.doi.org/10.1130/G31031.1.

Wagner, L.S., Fouch, M.J., James, D.E., Hanson-Hedgecock, S., 2012. Crust and upper mantle structure beneath the Pacific Northwest from joint inversions of ambient noise and earthquake data. Geochem. Geophys. Geosyst. 13 (1), Q0AN03. http://dx.doi.org/10.1029/2012GC004353.

Yuan, H., Romanowicz, B., Fischer, K.M., Abt, D., 2011. 3-D shear wave radially and azimuthally anisotropic velocity model of the North American upper mantle. Geophys. J. Int. 184, 1237–1260.

Zandt, G., Myers, S.C., Wallace, T.C., 1995. Crust and mantle structure across the Basin and Range–Colorado Plateau boundary at 37 N latitude and implications for Cenozoic extensional mechanism. J. Geophys. Res. 100 (B6), 10,529–10,548.

Zelt, C.A., White, D.J., 1995. Crustal structure and tectonics of the southeastern Canadian Cordillera. J. Geophys. Res. 100, 24,255–24,273.

Zelt, B.C., Clowes, R.M., Ellis, R.M., 1993. Crustal velocity structure in the eastern Insular and southernmost Coast belts, Canadian Cordillera. Can. J. Earth Sci., 30. University of British Columbia, Department of Geophysics and Astronomy, Vancouver, BC, Canada pp. 1014–1027.

Zhang, Q., Sandvol, E., Liu, M., 2009. Tomographic Pn velocity and anisotropy structure in the Central and Eastern United States. Bull. Seismol. Soc. Am. 99 (1), 422–427. http://dx.doi.org/10.1785/0120080246.